Journal of the American Heart Association

ORIGINAL RESEARCH

Inflammatory Role of Milk Fat Globule–Epidermal Growth Factor VIII in Age-Associated Arterial Remodeling

Leng Ni, MD, PhD*; Lijuan Liu, MD*; Wanqu Zhu, PhD; Richard Telljohann, MS; Jing Zhang, BS; Robert E. Monticone, MS; Kimberly R. McGraw, BS; Changwei Liu, MD; Christopher H. Morrell, PhD; Pablo Garrido-Gil, PhD; Jose Luis Labandeira-Garcia, MD, PhD; Edward G. Lakatta, MD; Mingyi Wang, MD, PhD

BACKGROUND: Age-associated aortic remodeling includes a marked increase in intimal medial thickness (IMT), associated with signs of inflammation. Although aortic wall milk fat globule–epidermal growth factor VIII (MFG-E8) increases with age, and is associated with aortic inflammation, it is not known whether MFG-E8 is *required* for the age-associated increase in aortic IMT. Here, we tested whether MFG-E8 is *required* for the age-associated increase in aortic IMT.

METHODS AND RESULTS: To determine the role of MFG-E8 in the age-associated increase of IMT, we compared aortic remodeling in adult (20-week) and aged (96-week) MFG-E8 (–/–) knockout and age matched wild-type (WT) littermate mice. The average aortic IMT increased with age in the WT from 50±10 to 70±20 μm (P<0.0001) but did not significantly increase with age in MFG-E8 knockout mice. Because angiotensin II signaling is implicated as a driver of age-associated increase in IMT, we infused 30-week-old MFG-E8 knockout and age-matched littermate WT mice with angiotensin II or saline via osmotic minipumps to determine whether MFG-E8 is required for angiotensin II–induced aortic remodeling. (1) In WT mice, angiotensin II infusion substantially increased IMT, elastic lamina degradation, collagen deposition, and the proliferation of vascular smooth muscle cells; in contrast, these effects were significantly reduced in MFG-E8 KO mice; (2) On a molecular level, angiotensin II treatment significantly increased the activation and expression of matrix metalloproteinase type 2, transforming growth factor beta 1, and its downstream signaling molecule phosphorylated mother against decapentaplegic homolog 2, and collagen type I production in WT mice; however, in the MFG-E8 knockout mice, these molecular effects were significantly reduced; and (3) in WT mice, angiotensin II increased the levels of aortic inflammatory markers phosphorylated nuclear factor-kappa beta p65, monocyte chemoattractant protein 1, tumor necrosis factor alpha, intercellular adhesion molecule 1, and vascular cell adhesion molecule 1 molecular expression, while in contrast, these inflammatory markers did not change in knockout mice.

CONCLUSIONS: Thus, MFG-E8 is required for both age-associated proinflammatory aortic remodeling and also for the angiotensin II–dependent induction in younger mice of an aortic inflammatory phenotype observed in advanced age. Targeting MFG-E8 would be a novel molecular approach to curb adverse arterial remodeling.

Key Words: age-associated aortic remodeling ■ angiotensin II signaling ■ inflammation ■ intimal medial thickening ■ milk fat globule–epidermal growth factor 8

Milk fat globule-epidermal growth factor VIII (MFG-E8) is a secreted extracellular glycoprotein that was initially discovered as a bridging molecule between apoptotic cells and macrophages for the clearance of cellular debris, also known as efferocytosis.[1,2] Recent studies have also shown that MFG-E8 exerts an inflammatory role in vascular remodeling.[3–9] In vivo studies have demonstrated that arterial MFG-E8

Correspondence to: Mingyi Wang, MD, PhD, FAHA, Laboratory of Cardiovascular Science, National Institution on Aging, National Institutes of Health, Biomedical Research Center (BRC), 251 Bayview Boulevard, Baltimore, MD 21224. Email: mingyiw@grc.nia.nih.gov

*L. Ni and L. Liu contributed equally.

Supplemental Material is available at https://www.ahajournals.org/doi/suppl/10.1161/JAHA.121.022574

For Sources of Funding and Disclosures, see page 12.

JAHA is available at: www.ahajournals.org/journal/jaha

CLINICAL PERSPECTIVE

What Is New?

- Milk fat globule–epidermal growth factor VIII increases with age and is required for age-associated proinflammatory arterial remodeling that results in aortic intimal medial thickening.
- In younger mice, milk fat globule–epidermal growth factor 8 is also essential for angiotensin II–induced adverse arterial remodeling that mimics that which occurs in advanced age via the increase of proinflammation, intimal medial thickening, elastin fragmentation, collagen deposition, and vascular smooth muscle cell proliferation.

What Are the Clinical Implications?

- Since milk fat globule–epidermal growth factor VIII is required for age-associated proinflammation in arterial wall remodeling, targeting milk fat globule–epidermal growth factor 8 is a potential molecular approach to curb inflammatory arterial remodeling, thus maintaining the health of the arterial system during aging and in arterial diseases such as hypertension.

Nonstandard Abbreviations and Acronyms

AT1	angiotensin II receptor type 1
AT2	angiotensin II receptor type 2
ICAM1	intercellular adhesion molecule 1
IMT	intimal medial thickness
MCP1	monocyte chemoattractant protein 1
MFG-E8	milk fat globule–epidermal growth factor VIII
MMP2	matrix metalloproteinase type 2
MT1MMP	memrane type I of MMP activator
NF-κB p65	nuclear factor-kappa beta p65
p-NF-κB p65	phosphorylated nuclear factor-kappa beta p65
SMAD2	smother against decapentaplegic homolog 2
TGF-β1	transforming growth factor beta 1
TNF-α	tumor necrosis factor alpha
VCAM1	vascular cell adhesion molecule 1
VSMC	vascular smooth muscle cell
WT	wild-type

protein levels increase during aging, arterial injury, and also in arterial walls of hypertensive, diabetic, and atherosclerotic animal models.[3–8,10,11] These studies suggest that MFG-E8 signaling plays an important role in the initiation and progression of adverse arterial remodeling such as intimal medial thickening.

Angiotensin II, a major metabolic component of the renin-angiotensin-aldosterone signaling system, produces multiple cardiovascular inflammatory effects.[12,13] Physiologically, angiotensin II signaling is critical in regulating blood pressure. In pathological conditions, angiotensin II stress signaling induces inflammation, contributing to the development of arterial aging and hypertensive vasculopathy.[12,14] Our previous study showed that younger adult animals infused with angiotensin II exhibited an older arterial phenotype, including increased intimal vascular smooth muscle cell (VSMC) infiltration, intimal medial thickening (IMT), matrix metalloproteinase type 2 (MMP2) activation, transforming growth factor beta 1 (TGF-β1) activation, and collagen deposition, eventually leading to elevated systolic blood pressure.[15] In vitro studies have demonstrated that MFG-E8 is a pivotal relay element within the angiotensin II/monocyte chemoattractant protein 1 (MCP1) signaling cascade that mediates VSMC inflammation, invasion, and proliferation.[3,4]

Although both MFG-E8 and angiotensin II increase in the inflamed aging arterial wall or in cultured aging VSMCs,[3,4] whether the underlying proinflammatory role of MFG-E8 is required for age-associated remodeling and aortic remodeling caused by angiotensin II remains unknown. We hypothesized that a chronic infusion of angiotensin II to younger mice, like younger rats,[15] would generate an "older" arterial inflammatory phenotype, which is impacted by MFG-E8 signaling. To this end, younger (30-week-old) wild-type (WT) and MFG-E8 knockout (–/–) (KO) mice infused with angiotensin II or saline were used and compared with untreated control mice with a wide range of ages (from 4 to 96 weeks) to investigate if MFG-E8 is necessary for angiotensin II–associated arterial inflammatory remodeling at the molecular, cellular, and tissue levels.

METHODS

All data, analytic methods, and study materials are available to other researchers for purposes of reproducing the results or replicating a procedure. The material that supports the findings of this study is available from the corresponding author upon reasonable request.

Experimental Animals

All experiments were conducted according to the protocols (445-LCS-2022) approved by the National Institute on Aging in accordance with the National Institutes of Health Animal Care and Use Committee. MFG-E8 (–/–)

knockout mice that were generated, characterized, and genotyped as described previously, were obtained from Dr. Mark Udey at the National Cancer Institute.[16,17] Transgenic Rip1-Tag2 mice were obtained from the National Cancer Institute. MFG-E8 knockout mice were generated by replacing exons 2 to 6 of the gene encoding MFG-E8 in 129SvJ embryonic cells with a neomycin-resistant cassette. Mice were genotyped by polymerase chain reaction using the following primers: Rip1-Tag2, GGACAAACCACAACTAGAATGCAGTG (forward) and CAGAGCAGAATTGTGGAGTGG (reverse); Neo, GCCAGAGGCCACTTGTGTAG; and MFG-E8, CTCTCAGATTCACCTGCTCGTG and CACCGTTCAG GCACAGGCTG. Thirty-week-old male MFGE8 knockout mice (homozygous for lack of MFG-E8) and age-matched WT mice were used in this angiotensin II infusion study. In addition, 4-, 8-, 20, 50-, and 96-week-old male WT and age-matched knockout archival aortic sections or frozen tissue were used for the study of age-related arterial remodeling.

Angiotensin II Infusion

Osmotic mini-pumps (Alzet Model 2004) were implanted dorsally and subcutaneously in anesthetized (2% isoflurane) mice (n=14–18/group) to deliver angiotensin II (500 ng/kg per min) or 0.9% saline (placebo) for 28 days.

Sample Collection and Preparation

Blood Collection

Ocular blood was collected at 14 days after mini-pump implantation. At the end of the experiment, mice were euthanized under sodium pentobarbital anesthesia, and blood was collected from the right atrium into a 4-mL EDTA-coated Eppendorf tube immediately. The blood samples were centrifuged for 15 minutes at 3000 rpm (1500*g*) at 4 °C. The supernatant was carefully transferred into a 0.5-mL Eppendorf tube and stored at −80 °C until use.

Tissue Collection

Tissue samples were isolated from the ascending aorta to the bifurcation of the common iliac artery of mice. For morphological analysis, animals were perfused with 4% paraformaldehyde- PBS at physiological pressure for 5 minutes; and aortic tissues were paraffin-embedded and sectioned for histological analysis. For western blotting, animals were perfused with 0.9% saline and fresh aortic tissues were snap-frozen in liquid nitrogen and stored at −80 °C until use.

Histology, Immunostaining, and Morphometric Analyses

To quantitate aortic remodeling, IMT was measured using hematoxylin and eosin staining; elastin breaks were counted via Elastin Verhoeff's–Van Gieson staining; and collagen deposition was evaluated with Masson's trichrome staining. Hematoxylin and eosin, Elastin Verhoeff's–Van Gieson, and Masson trichrome staining were performed using MasterTech stain kits (StatLab, McKinney, TX). Staining of aortic walls was performed as described in previous studies.[18] In brief, aortic paraffin sections (5 μm in thickness) were used for immunostaining with antiproliferating cellular nuclear antigen, tissue necrosis factor-alpha (TNF-α), intercellular adhesion molecule 1 (ICAM1), vascular cell adhesion molecule 1 (VCAM1), and collagen type I antibodies. Details of primary antibodies used are listed in Table 1. The ratios of target immunohistochemical staining positive area to the total tissue or cell area were determined via a computer-imaging program according to the instruction provided by manufacture (MetaMorph Imaging System; Molecular Devices, San Jose, CA).

Western Blotting

Western blot analysis was performed as described previously.[18] In brief, total protein was quantified using the Pierce Coomassie (Bradford) protein assay kit (Hercules, CA), following the manufacturer's instructions. Ten micrograms of total protein was run on 4% to 12% NuPAGE gels (Thermo Fisher Scientific, Waltham, MA), then transferred to a polyvinylidene fluoride membrane and immunoblotted with the antibodies listed in Table 1. Western blotting bands were quantified using National Institutes of Health image J (http://rsb.info.nih.gov/nih-image/) and the intensity values were normalized to loading control GAPDH or β-actin.

PAGE Zymography

MMP-2 activity was determined via PAGE gelatin zymography (Thermo Fisher Scientific) as described previously.[19]

Angiotensin II Quantification

RayBio Mouse Angiotensin II ELISA kit, a commercially available ELISA (RayBiotech Life, Peachtree Corners, GA) was used to measure the amount of angiotensin II in mouse plasma.

Statistical Analysis

All data were presented as mean±SEM. Statistical analyses used 1-way, 2-way, or 2-way repeated-measures ANOVA followed by Bonferroni post hoc tests used for multiple comparisons. These statistical analyses were performed using Prism version 8.4.1 (GraphPad Software, San Diego, CA). For systolic blood pressure, the repeated-measures data were also analyzed using a linear mixed-effects model.[20] A value of $P \leq 0.05$ was considered statistically significant. Supplemental materials and methods can be found in Data S1.

Table 1. Primary Antibodies

Antibody	Company	Catalog no.	Titer for WB	Titer for IHC
Angiotensin II	Sigma	A9525		1:350
AT1	Santa Cruz	sc-515 884	1:500	1:100
AT2	Abcam	Ab92445	1;1000	1:100
Collagen I	Santa Cruz	sc-59 772		1:50
GAPDH	Cell Signaling technology	5014	1:1000	
ICAM1	Santa Cruz Biotechnology	Sc-8439		1:50
MCP1	R&D Systems	AF479	1:200	
MFG-E8	R&D Systems	AF2805	1:1000	
MMP2	R&D Systems	AF1488	1:500	
MT1-MMP	Thermo Fisher Scientific	PA5-16514	1:500	
NF-κB p65	Santa Cruz Biotechnology	sc-8008	1:500	
p-NF-κB p65	Santa Cruz	Sc-33 020	1:500	1:50
PCNA	Santa Cruz	sc-9857		1:50
p-Smad2	Santa Cruz Biotechnology	3108	1:500	
Smad2	Santa Cruz Biotechnology	5339	1:1000	
TGF-β1	Santa Cruz Biotechnology	sc-146	1:200	
TNF-α	Abcam	ab9739	1:1000	1:100
VCAM1	Santa Cruz Biotechnology	Sc-13 160		1:50

AT1 indicates angiotensin II receptor type 1; AT2, angiotensin II receptor type 2; ICAM1, intercellular adhesion molecule 1; IHC immunohistochemistry; MCP1, monocyte chemoattractant protein 1; MMP2, matrix metalloproteinase type 2; MT1MMP, member type I of MMP activator; NF-κB p65, nuclear factor-kappa beta p65; p-NF-κB p65, phosphorylated nuclear factor-kappa beta p65; PCNA, proliferating cell nuclear antigen; SMAD2, mother against decapentaplegic homolog 2; p-SMAD2 phosphorylated smother against decapentaplegic homolog 2; TGF-β1, transforming growth factor beta 1; TNF-α tumor necrosis factor alpha; VCAM1, vascular cell adhesion molecule 1; and WB, western blotting.

RESULTS

Age-Associated Increase in IMT Does Not Occur in MFG-E8 Knock-Out Mice

To determine the role of MFG-E8 in the age-associated increase of IMT, we compared aortic remodeling in adult (20-week) and aged (96-week) MFG-E8 knockout and age-matched WT littermate mice. We confirmed that aortic MFG-E8 protein was markedly elevated in untreated 50-week-old versus 8-week-old WT mice but was not detected in knockout mice (Figure 1A). The average aortic IMT increased with age in the WT from 50±10 to 70±20 (P<0.0001) but did not significantly increase with age in MFG-E8 knockout mice (Figure 1B). In 96-week-old untreated WT, aortic IMT was markedly increased versus 20-week-old, but no aging increase was observed in the KO mouse (Figure 1B).

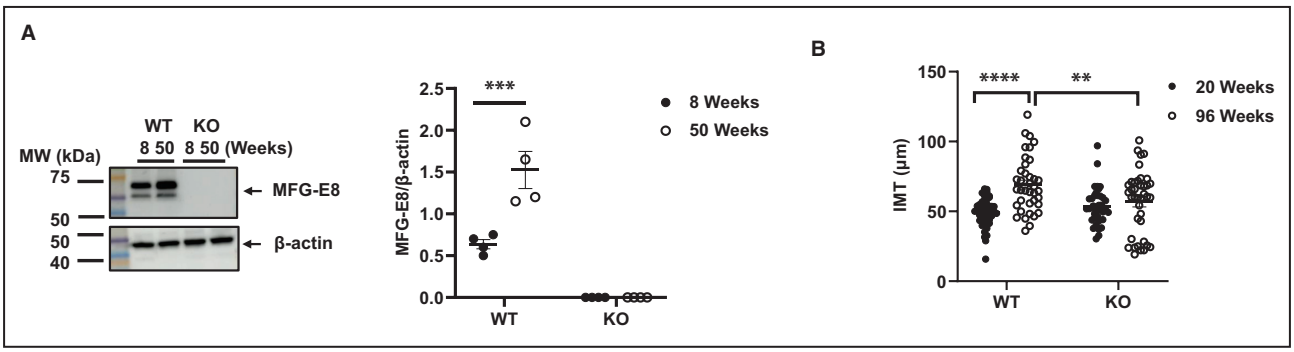

Figure 1. Age-associated characteristics of the MFG-E8 knockout mouse.
A, Representative western blots of aortic MFG-E8 (left panel). Quantitative data of western blots show aortic MFG-E8 protein abundance (P<0.01 for main age effect, P<0.0001 for main genotype effect, P<0.01 for age×genotype, by 2-way ANOVA). Graph (right panel) showing mean±SEM combined with individual data points for knockout and WT mice. ***P<0.001 by Bonferroni post hoc tests following 2-way ANOVA. **B**, Morphometric analysis of the aortic IMT (P<0.0001 for main age effect, P<0.01 for main genotype effect, P<0.0001 for interaction by 2-way ANOVA). Graph showing mean±SEM combined with individual data points for knockout and WT mice. **P<0.01; and ****P<0.0001 by Bonferroni post hoc tests following 2-way ANOVA. IMT indicates intimal medial thickness; KO, knockout; MFG-E8, milk fat globule–epidermal growth factor VIII; MW, molecular weight; and WT, wild-type.

In addition, aortic angiotensin II protein was significantly increased in untreated aging WT mice, but not in the MFG-E8 KO (Figure S1A). Immunostaining demonstrated that the angiotensin II receptor type 1 (AT1) was markedly increased in the aortic walls of older untreated WT and relatively reduced in the older MFG-E8 KO (Figure S1B); and the angiotensin II receptor type 2 (AT2) was decreased in both aging WT and KO aortic walls (Figure S1C). We confirmed the immunostaining AT1 aging effect with western blot analysis and observed no significant AT2 decrease in aging MFG-E8 KO mice (Figure S1D). Notably, aortic MFG-E8 protein levels were significantly decreased in the AT1 knockout mouse, but these levels were not altered in the AT2 knockout mouse (Figure S2) suggesting that MFG-E8 modulates age-associated adverse arterial remodeling and angiotensin II/AT1 signaling.

MFG-E8 Is Required for the Angiotensin II–Induced Aortic Remodeling That Accompanies Advanced Age

Because angiotensin II signaling is implicated as a driver of age-associated increase in IMT, we infused 30-week-old MFG-E8 knockout mice and age-matched littermate WT mice with angiotensin II or saline via osmotic mini-pumps to determine whether MFG-E8 is required for angiotensin II induced aortic remodeling. Compared with saline, angiotensin II infusion markedly increased the levels of circulating angiotensin II in both WT and KO mice accessed on days 14 and 28, to an even greater extent in MFG-E8 KO than in WT (Figure 2A). Angiotensin II infusion increased the AT1 receptor expression and reduced the AT2 receptor in both genotypes (Figure 2B and 2C). Angiotensin II dramatically increased the expression of aortic MFG-E8 in WT mice, but aortic MFG-E8 protein was not detectable in the knockout mice infused with either angiotensin II or saline (Figure 2D).

Immunohistochemistry of mouse aortic walls was performed after 4 weeks of angiotensin II or saline infusion. The morphometrical analysis indicated that adverse arterial remodeling was dependent upon the presence of MFG-E8. In WT mice, a marked increase in IMT was observed in the aortic walls of mice infused with angiotensin II compared with saline; however, in knockout mice, no significant difference in IMT was observed (Figure 3A). Elastin Verhoeff's–Van Gieson staining indicated a significant increase in the number of the elastin fiber breaks in WT mice treated with angiotensin II versus saline, while this effect was substantially reduced in knockout mice (Figure 3B). In WT mice infused with angiotensin II, Masson's trichrome staining showed that the fraction of intimal medial extracellular matrix, mainly collagen, was increased versus saline, while this effect was not observed in knockout mice (Figure 3C). VSMC proliferation is a key cellular event of arterial thickening in hypertension induced by angiotensin II.[21] In WT mice infused with angiotensin II, the percentage of proliferating cell nuclear antigen (PCNA)–positive VSMCs, an index of cellular division, was markedly elevated when compared with saline; however, no difference in proliferating cell nuclear antigen was seen in knockout animals (Figure 3D). Thus, MFG-E8 plays a necessary role in angiotensin II-induced IMT, elastic lamina degradation, collagen deposition, and proliferation of VSMCs; and in general, MFG-E8 deficiency alleviates these effects in aortic walls.

Angiotensin II Activation of Aortic MMP2 Is Dependent on MFG-E8

Prior studies indicate that increased levels of MMP2 protein and MMP2 activation occur in response to angiotensin II signaling.[15] PAGE zymography demonstrated that the levels of activated MMP2 within the aortic walls of younger mice after angiotensin II infusion were dependent upon the presence of MFG-E8 (Figure 4A): in WT mice, angiotensin II infusion markedly increased the levels of activated aortic MMP2 compared with saline; in KO mice, activated MMP2 in angiotensin II infused animals was significantly higher than saline, but was still significantly less than that of the angiotensin II–treated WT mice (Figure 4A). Western blot analysis showed that the abundance of aortic MMP2 protein induced by angiotensin II was dependent upon the presence of MFG-E8 (Figure 4B): in WT mice, angiotensin II markedly increased the levels of MMP2 protein in aortic walls when compared with saline (Figure 4B middle panel); in knockout mice, the MMP2 protein levels were significantly increased in angiotensin II– versus saline-treated mice but was significantly less than that of angiotensin II–treated WT mice (Figure 4B middle panel). Similarly, angiotensin II increased the levels of member type I of MMP activator (MT1MMP), an activator of MMP2, and was dependent on the presence of MFG-E8 (Figure 4B, right panel); in WT mice, angiotensin II significantly increased the levels of MT1MMP protein in the aortic wall when compared with saline; however, in knockout animals, there was no significant increase in MT1MMP protein levels (Figure 4B, right panel). MFG-E8 is necessary for the increased activation and expression of MMP2 induced by angiotensin II in the aortic walls of younger animals.

Angiotensin II Increases Aortic TGF-β1 Fibrotic Signaling Through MFG-E8

Angiotensin II signaling and increased MMP2 activation, all promote the activation of TGF-β1 and its fibrotic effect within arterial walls in vivo and in cultured VSMCs.[15,22,23] Western blotting analysis demonstrated

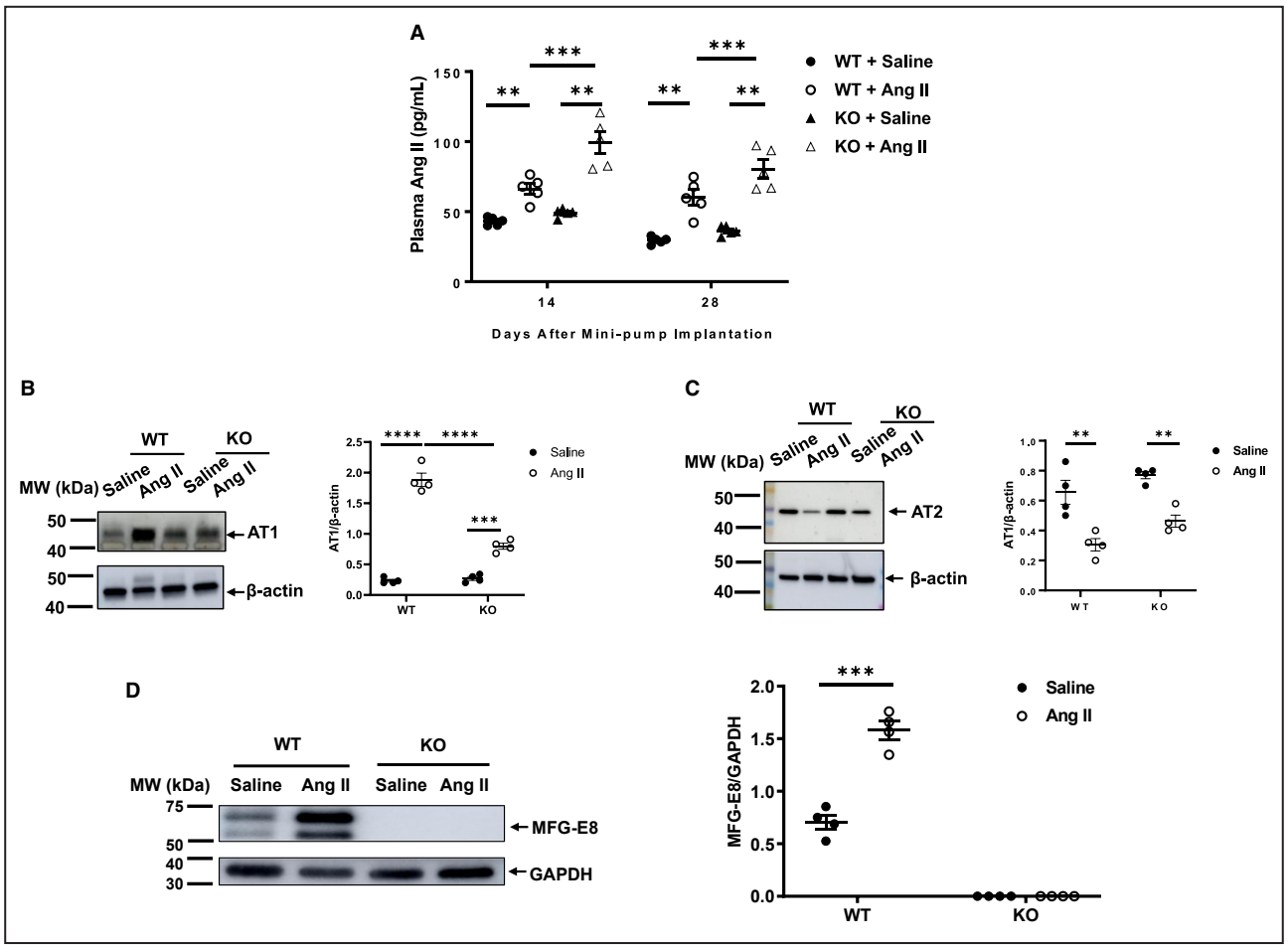

Figure 2. MFG-E8 is required for the angiotensin II–induced signaling.
A, Plasma angiotensin II concentrations (P<0.001 for overall treatment effect by repeated 2-way ANOVA with the factors of treatment and genotype). Graph showing mean±SEM with individual animal data from knockout and WT mice with angiotensin II or saline infusion over time. **P<0.01 and ***P<0.001 by Bonferroni post hoc tests following 2-way ANOVA. **B**, Representative western blots of AT1 receptors (left panel). Western blotting analysis of the AT1 abundance (P<0.0001 for main angiotensin II treatment effect, P<0.0001 for main genotype effect, P<0.0001 for treatment×genotype, by 2-way ANOVA). Graph (right panel) showing mean±SEM combined with individual data points for knockout and WT mice. ***P<0.001 and ****P<0.0001 by Bonferroni post hoc tests following 2-way ANOVA. **C**, Representative western blots of AT2 receptor (left panel). Western blotting analysis of the AT2 abundance (P<0.001 for main angiotensin II infusion effect, P<0.05 for main genotype effect by 2-way ANOVA). Graph (right panel) showing mean±SEM combined with individual data points for knockout and WT mice. **P<0.01 by Bonferroni post hoc tests following 2-way ANOVA. **D**, Representative western blots of aortic MFG-E8 (left panel). Quantitative data of western blots of aortic MFG-E8 protein abundance as normalized by GAPDH (P<0.001 for main angiotensin II infusion effect, P<0.001 for main genotype effect, P<0.001 for treatment×genotype, by 2-way ANOVA). Graph (right panel) showing mean±SEM with individual data for knockout and WT mice with angiotensin II or saline infusion. ***P<0.001 by Bonferroni post hoc tests following 2-way ANOVA. Ang II indicates angiotensin II; AT1, angiotensin II receptor type 1; AT2, angiotensin II receptor type 2; KO, knockout; MFG-E8, milk fat globule–epidermal growth factor VIII; MW, molecular weight; and WT, wild-type.

that the angiotensin II-induction of activated arterial TGF-β1 and it's signaling was dependent upon the presence of MFG-E8 (Figure 5A and 5B): in WT mice, angiotensin II infusion markedly increased the levels of activated TGF-β1 protein in the aortic walls; while in knockout mice there was a smaller increase when compared with saline (Figure 5A and 5B). Notably, in angiotensin II–infused mice, the levels of TGF-β1 protein in the WT mice was significantly higher than those found in knockout mice (Figure 5A and 5B). Similarly, western blot analysis demonstrated that angiotensin II infusion increased SMAD2 phosphorylation, a TGF-β1 downstream signaling molecule, and was also dependent upon the presence of MFG-E8 (Figure 5A and 5B). In WT mice, angiotensin II infusion markedly increased the levels of activated phosphorylated SMAD2 protein in the aortic walls compared with saline; in contrast, in knockout mice, there was no significant increase of these proteins with angiotensin II infusion (Figure 5A and 5B). Expectedly, immunohistostaining and western blotting

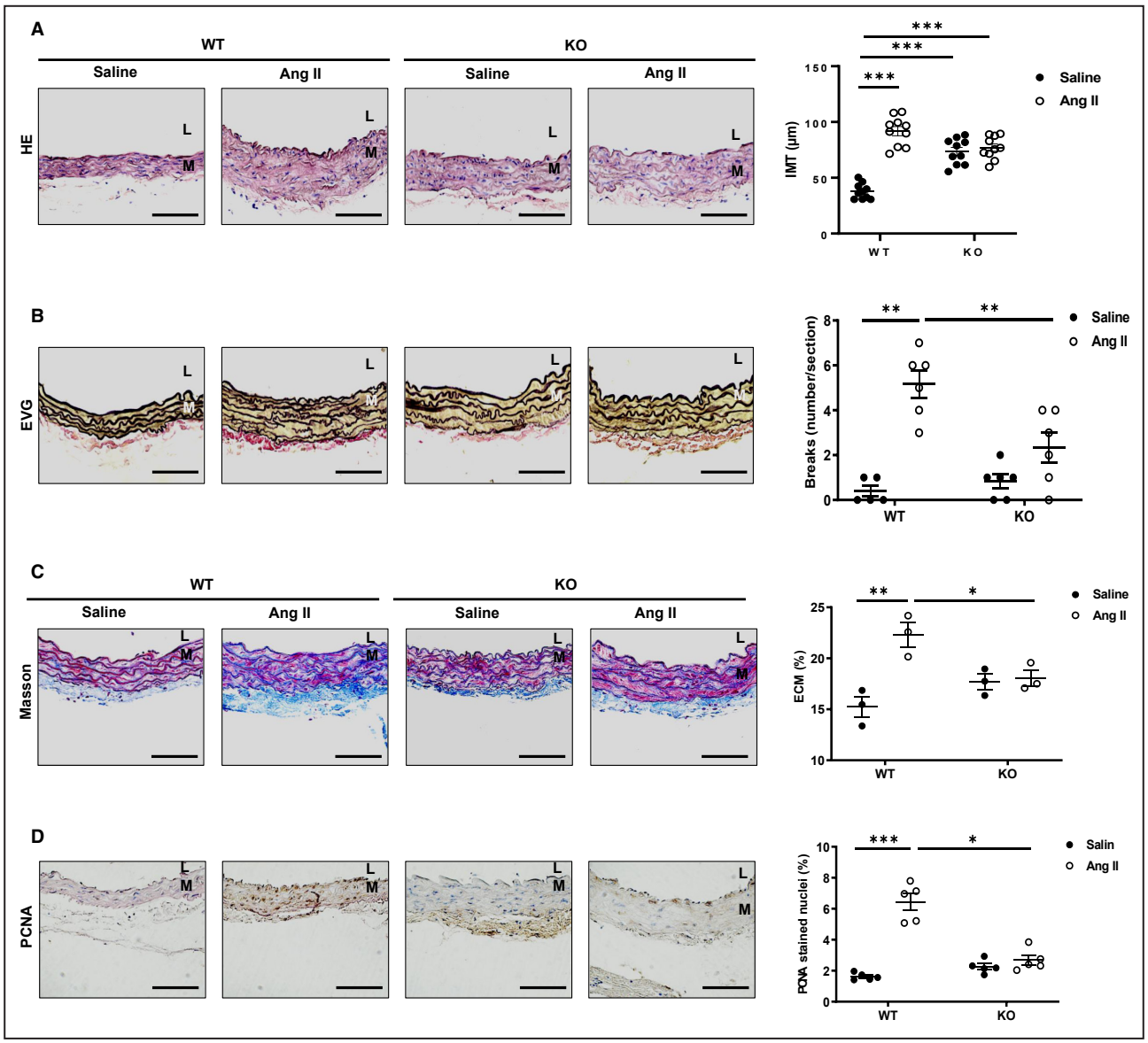

Figure 3. MFG-E8 is required for the angiotensin II–induced aortic remodeling.
A, Photomicrographs of hematoxylin and eosin staining of aortic walls. Morphometric analysis of the aortic IMT (P<0.001 for main treatment effect, P<0.001 for main genotype effect, P<0.001 for treatment×genotype, by 2-way ANOVA) (far right panel) **B**, Photomicrographs of EVG staining of aortic walls. Quantification of elastin breaks (P<0.05 for main treatment effect, P<0.001 for main genotype effect, P<0.01 for treatment×genotype, by 2-way ANOVA) (far right panel). **C**, Photomicrograph of Masson's trichrome staining of aortic walls. Morphometric analysis of intimal medial ECM (blue color) (P>0.05 for main treatment effect, P<0.01 for main genotype effect, P<0.01 for treatment×genotype, by 2-way ANOVA) (far right panel). **D**, Photomicrographs of PCNA immunostaining of aortic walls. Quantification of relative PCNA stained nuclei area (P>0.05 for main treatment effect, P<0.01 for main genotype effect, P<0.01 for treatment×genotype, by 2-way ANOVA) (far right panel). Graph showing mean±SEM with individual animal data points for knockout and WT mice with angiotensin II or saline infusion. *P<0.05, **P<0.01 and ***P<0.001 by Bonferroni post hoc tests following 2-way ANOVA. Scale bar=100 μm. Ang II indicates angiotensin II; ECM, extracellular matrix; EVG, Elastin Verhoeff's–Van Gieson; HE, hematoxylin and eosin; IMT, intimal medial thickness; KO, knockout; L, lumen; M, media; PCNA, proliferating cell nuclear antigen; and WT, wild-type.

analyses indicated that the angiotensin II induction of the arterial collagen I levels, a TGF-β1/ phosphorylated SMAD2 downstream signaling product, was dependent upon MFG-E8 (Figure 5C and 5D). In WT mice, angiotensin II infusion markedly increased the levels of collagen type I protein in the aortic walls when compared with saline; in contrast, in knockout mice, there was no significant increase of collagen type I when treated with angiotensin II (Figure 5C and 5D). Thus, MFG-E8 plays a necessary role in the angiotensin II–induced activation of TGF-β1, its downstream signaling molecule, phosphorylated SMAD2, and collagen I in the aortic wall of mice.

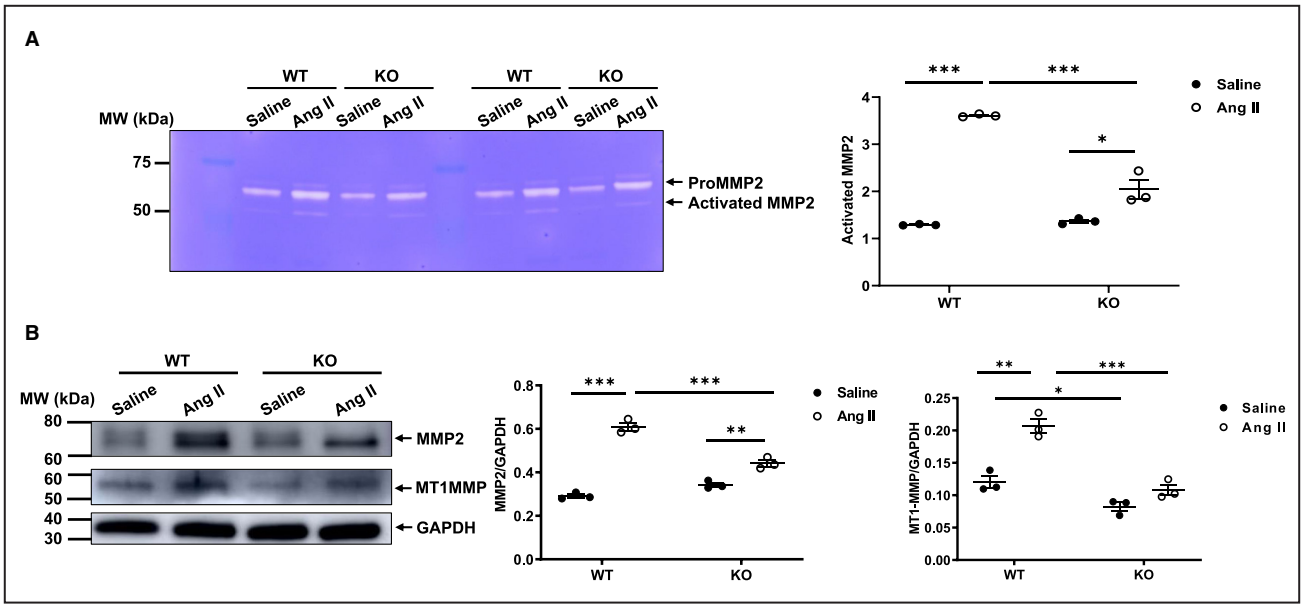

Figure 4. Angiotensin II activation of aortic MMP2 is dependent on MFG-E8.
A, Representative zymograms of aortic gelatinases (left panel). Quantitative graph shows activated MMP2 protein abundance ($P<0.001$ for main treatment effect, $P<0.001$ for main genotype effect, $P<0.001$ for treatment×genotype, by 2-way ANOVA). Graph (right panel) showing mean±SEM with individual data for knockout and WT mice with angiotensin II or saline infusion. *$P<0.05$ and ***$P<0.001$ by Bonferroni post hoc tests following 2-way ANOVA. **B**, Representative western blots of aortic MMP2, MT1MMP, and GAPDH (left panel). Quantitative data of aortic MMP2 protein abundance ($P<0.001$ for main treatment effect, $P<0.01$ for main genotype effect, $P<0.01$ for treatment×genotype, by 2-way ANOVA) (middle panel). Quantitative data of aortic MT1MMP2 protein abundance ($P<0.001$ for main treatment effect, $P<0.01$ for main genotype effect, $P<0.01$ for treatment×genotype, by 2-way ANOVA). Graph (right panel) showing mean±SEM with individual data for knockout and WT mice with angiotensin II or saline infusion. *$P<0.05$, **$P<0.01$, and ***$P<0.001$ by Bonferroni post hoc tests following 2-way ANOVA. Ang II indicates angiotensin II; IMT, intimal medial thickness; KO, knockout; MFG-E8, milk fat globule–epidermal growth factor VIII; MMP2, matrix metalloproteinase type 2; MT1MMP, membrane type I of MMP activator; MW, molecular weight; and WT, wild-type.

Angiotensin II Activation of Nuclear Factor-Kappa Beta Signaling and Its Downstream Proinflammatory Effects Require MFG-E8

Nuclear factor-kappa beta (NF-κB) is a prominent proinflammatory transcription factor in inflamed arterial walls.[24,25] NF-κB p65, an element of NF-κB activation, facilitates the upregulation of its downstream inflammatory factors, MCP1, tissue necrosis factor-alpha 1 (TNF-α), ICAM1, and VCAM1, which are directly involved in the process of arterial inflammation.[25–27] Aging markedly increased aortic phosphorylated nuclear factor-kappa beta p65 (p-NF-κB p65) in the aging WT mice but did not increase in the knockout mice (Figure S3A and S3B).

Western blot analyses showed that the abundance of arterial p-NF-κB p65 in mice infused with angiotensin II was dependent on the presence of MFG-E8: p-NF-κB p65 protein abundance was markedly upregulated in WT mice infused with angiotensin II versus saline, whereas the protein levels remained at similar levels in both groups of knockout animals (Figure 6A and 6B). Western blotting analysis indicated that the abundance of aortic MCP1 protein induced by angiotensin II in mice was also dependent upon the presence of MFG-E8: WT mice infused with angiotensin II showed a significant increase in the levels of activated MCP1 protein in the aortic wall when compared with saline; conversely, knockout mice infused with angiotensin II exhibited similar levels of MCP1 protein expression when compared to saline (Figure 6A and 6C). Notably, when mice were treated with angiotensin II, MCP1 protein levels were significantly lower in knockout versus WT mice (Figure 6A and 6C). Western blotting and immunostaining analyses also revealed that angiotensin II infusion altered TNF-α protein levels in mice and was dependent upon MFG-E8: The level of TNF-α protein in WT mice was significantly increased in the aortic wall when infused with angiotensin II and compared with saline; however, the protein levels in knockout mice were not significantly altered in either treatment group (Figure 6A, 6D and 6E). In addition, immunohistostaining and morphometric analysis demonstrated that the increased levels of arterial adhesive molecules ICAM1 and VCAM1 protein in mice treated with angiotensin II

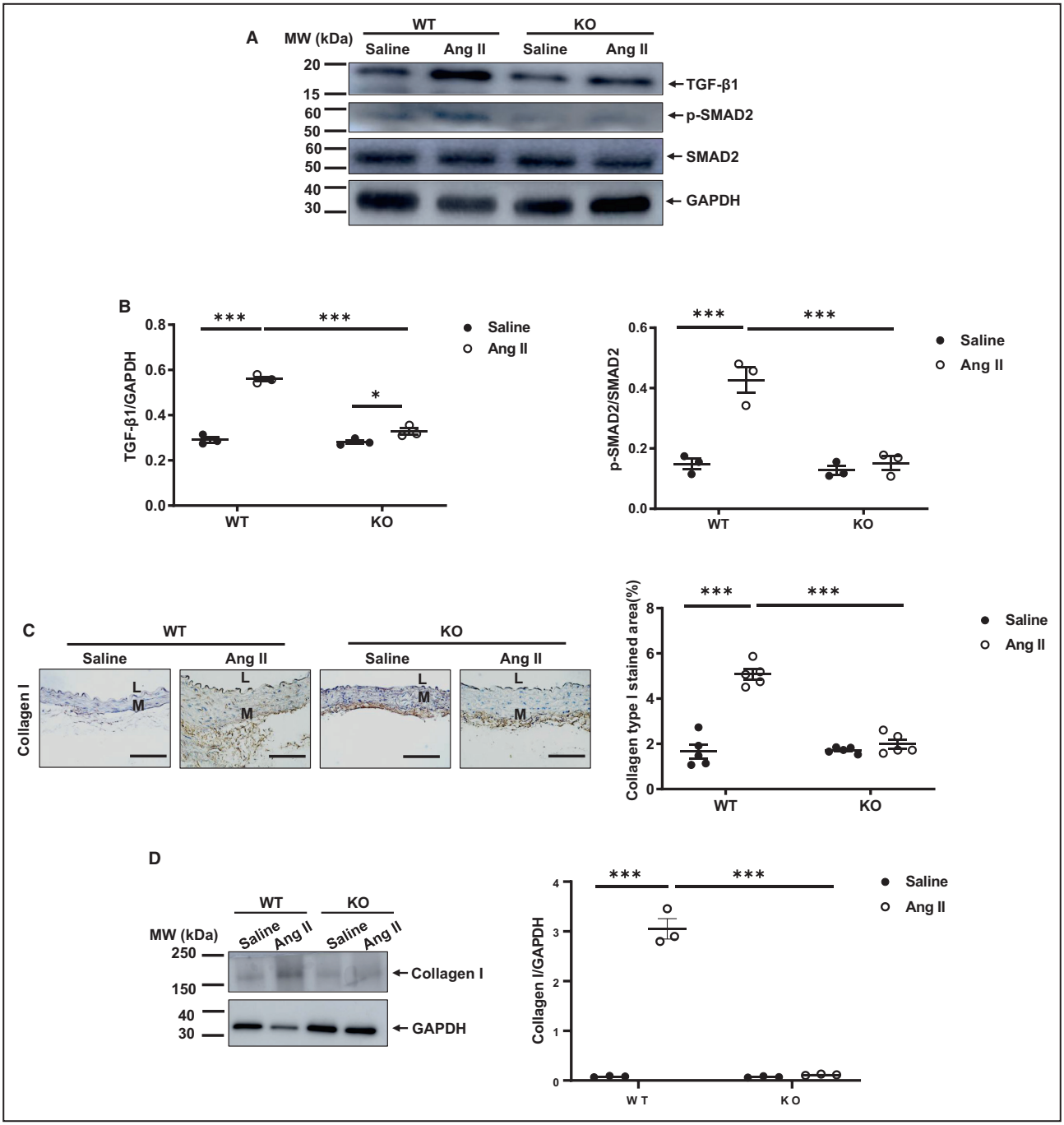

Figure 5. Angiotensin II increases aortic TGF-β1 fibrotic signaling through MFG-E8.
A, Representative western blots of aortic TGF-β1, p-SMAD2, and SMAD2. **B**, Quantitative data of aortic activated TGF-β1 protein abundance (P<0.001 for main treatment effect, P<0.001 for main genotype effect, P<0.001 for treatment×genotype, by 2-way ANOVA) (left panel). Quantitative data of aortic p-SMAD2/SMAD2 ratio (P<0.001 for main treatment effect, P<0.001 for main genotype effect, P<0.01 for treatment×genotype, by two-way ANOVA). Graph (right panel) showing mean±SEM with individual data for knockout and WT mice with angiotensin II or saline infusion. *P<0.05 and ***P<0.001 by Bonferroni post hoc tests following 2-way ANOVA. **C**, Photomicrographs of immunostaining collagen type I. Morphometric analysis shows relative collagen I immunostaining area (%) (P<0.001 for main treatment effect, P<0.001 for main genotype effect, P<0.001 for treatment×genotype, by 2-way ANOVA). Graph (far right panel) showing mean±SEM with individual data for knockout and WT mice with angiotensin II or saline infusion. ***P<0.001 by Bonferroni post hoc tests following 2-way ANOVA. **D**, Representative western blots of aortic collagen I. Quantitative data of aortic collagen I (P<0.01 for main treatment effect, P>0.05 for main genotype effect, P<0.0001 for treatment×genotype, by 2-way ANOVA). Graph (right panel) showing mean±SEM with individual data points for knockout and WT mice with angiotensin II or saline infusion. ***P<0.001 by Bonferroni post hoc tests following 2-way ANOVA. Scale bar=100 μm. Ang II indicates angiotensin II; KO, knockout; L, lumen; M, media; MW, molecular weight; p-SMAD2, phosphorylated mother against decapentaplegic homolog 2; SMAD2, s mother against decapentaplegic homolog 2; TGF-β1, transforming growth factor beta 1; and WT, wild-type.

were also dependent upon MFG-E8 (Figure 6G, 6H, 6I and 6J). In WT mice, angiotensin II infusion markedly increased the protein levels of both ICAM1 and VCAM1 in the aortic wall when compared with saline; however, in knockout mice, angiotensin II infusion did not significantly alter either ICAM1 or VCAM1 protein abundance versus saline (Figure 6G, 6H, 6I and 6J). MFG-E8 is required for angiotensin II–induced increases in p-NF-κB p65, both MCP-1, TNF-α, ICAM1, and VCAM1 protein expression in aortic walls. In addition, also see supplemental results in Data S2.

DISCUSSION

Role of MFG-E8 in Age-Associated Aortic Remodeling

The primary objective of this study was to determine the requirement of MFG-E8 in age-associated aortic inflammation and structural remodeling. The general strategy we employed was to age MFG-E8 knockout mice, and their WT littermates, to determine whether aortic inflammation and arterial wall thickening in old KO differed from that in old WT. Our first major finding was that MFG-E8 was indeed required for adverse aortic remodeling that accompanies advanced age, because the hallmarks or the extent of this remodeling, that is, inflammation and intimal medial thickening that were present in WT mice at 96 weeks of age were not observed in age-matched MFG-E8 KO mice, in which MFG-E8 was not expressed. However, it is noteworthy that IMT increased between 20 to 30 weeks of age in the KO mice but not in the WT mice (Figure 1B versus Figure 3A), and the elucidation of this unexpected phenotypic characteristic of the MFG-E8 knockout mice that occurred between 20 and 30 weeks merits further study. Nevertheless, in advanced age (96 weeks), the IMT of the MFG-E8 knockout mice was substantially reduced compared with age-matched WT mice (Figure 1B).

Role of MFG-E8 in Angiotensin II–Induced Aortic Remodeling

It is well documented that aortic angiotensin II increases with advancing age, and that angiotensin II is the quintessential perpetrator of age-associated adverse aortic remodeling. The marked increase in arterial wall MMP2 activation in WT mice in response to angiotensin II infusion is attributable, in part at least, to an angiotensin II–induced increase of MT1MMP, an activator of MMP2. We previously observed that treating VSMCs with recombinant human MFG-E8 activates MMP2,[28,29] suggesting that MFG-E8 is necessary for angiotensin II associated MMP2 activation. Notably, active MMP2 has a high capacity to degrade aortic elastin laminae, releasing activated TGF-ß1.[15,22,23,30]

Angiotensin II infusion induces the activation of aortic MMP2 and TGF-ß1, which promotes arterial elastic fiber degeneration and fibrosis and is dependent on MFG-E8. In addition, MMP2, a potent activator of latent TGF binding protein, facilitates the conversion from the latent to the active form of TGF-ß1.[22] We had previously demonstrated that treating VSMCs with recombinant human MFG-E8 increases the fibrogenic TGF-ß1/SMAD2/collagen type I signaling cascade in VSMCs.[28] Thus, this also suggested that MFG-E8 may be vital for angiotensin II–induced MMP2 activation/

Figure 6. Angiotensin II activation of NF-κB signaling and its downstream proinflammatory effects require MFG-E8.
A, Representative western blots of aortic p-NF-κB p65, NF-κB p65, MCP-1, TNF-α, and GAPDH. **B**, Quantitative data of p-NF-κB p65 protein abundance ($P<0.001$ for main treatment effect, $P<0.01$ for main genotype effect, $P<0.001$ for treatment×genotype, by 2-way ANOVA). Graph showing mean±SEM and individual data points for knockout and WT mice with angiotensin II or saline infusion. $^{**}P<0.01$ and $^{***}P<0.001$ by Bonferroni post hoc tests following 2-way ANOVA. **C**, Quantitative data of MCP1 protein abundance ($P<0.01$ for main treatment effect, $P<0.05$ for main genotype effect, $P<0.001$ for treatment×genotype, by two-way ANOVA). Graph showing mean±SEM with individual data points for knockout and WT mice with angiotensin II or saline infusion. $^{***}P<0.001$ by Bonferroni post hoc tests following two-way ANOVA. **D**, Quantitative data of TNF-α protein abundance ($P<0.001$ for main treatment effect, $P>0.05$ for main genotype effect, $P<0.05$ for treatment×genotype, by two-way ANOVA). Bar graph showing mean±SEM with individual data points for knockout and WT mice with angiotensin II or saline infusion. $^{***}P<0.001$ by Bonferroni post hoc tests following 2-way ANOVA. **E**, Photomicrographs of immunostaining of TNF-α. **F**, Quantitative data of aortic TNF-α immunostaining area (%) ($P<0.01$ for main treatment effect, $P<0.05$ for main genotype effect, $P<0.01$ for treatment×genotype, by two-way ANOVA). Graph showing mean±SEM with individual data for KO and WT mice with angiotensin II or saline infusion. $^{*}P<0.05$, $^{**}P<0.01$, and $^{***}P<0.001$ by Bonferroni post hoc tests following two-way ANOVA. **G**, Photomicrographs of immunostaining ICAM1. **H**, Morphometric analysis of relative ICAM1 immunostaining area (%) ($P<0.001$ for main treatment effect, $P<0.001$ for main genotype effect, $P<0.001$ for treatment×genotype, by 2-way ANOVA). Graph showing mean±SEM with individual data for knockout and WT mice with angiotensin II or saline infusion. $^{***}P<0.001$ by Bonferroni post hoc tests following 2-way ANOVA. **I**, Photomicrographs of immunostaining VCAM1. **J**. Morphometric analysis of relative VCAM1 immunostaining area (%) ($P<0.001$ for main treatment effect, $P<0.001$ for main genotype effect, $P<0.001$ for treatment×genotype, by two-way ANOVA). Graph showing mean±SEM with individual data for knockout and WT mice with angiotensin II or saline infusion. $^{***}P<0.001$ by Bonferroni post hoc tests following 2-way ANOVA. Scale bar=100 μm. Ang II indicates angiotensin II; ICAM1, intercellular adhesion molecule 1; KO, knockout; L, lumen; M, media; MCP1, monocyte chemoattractant protein 1; MFG-E8, milk fat globule–epidermal growth factor VIII; MW, molecular weight; NF-κB p65, nuclear factor-kappa beta p65; p-NF-κB p65, phosphorylated nuclear factor-kappa beta p65; VCAM1, vascular cell adhesion molecule 1; TNF-α, tumor necrosis factor alpha; and WT, wild-type.

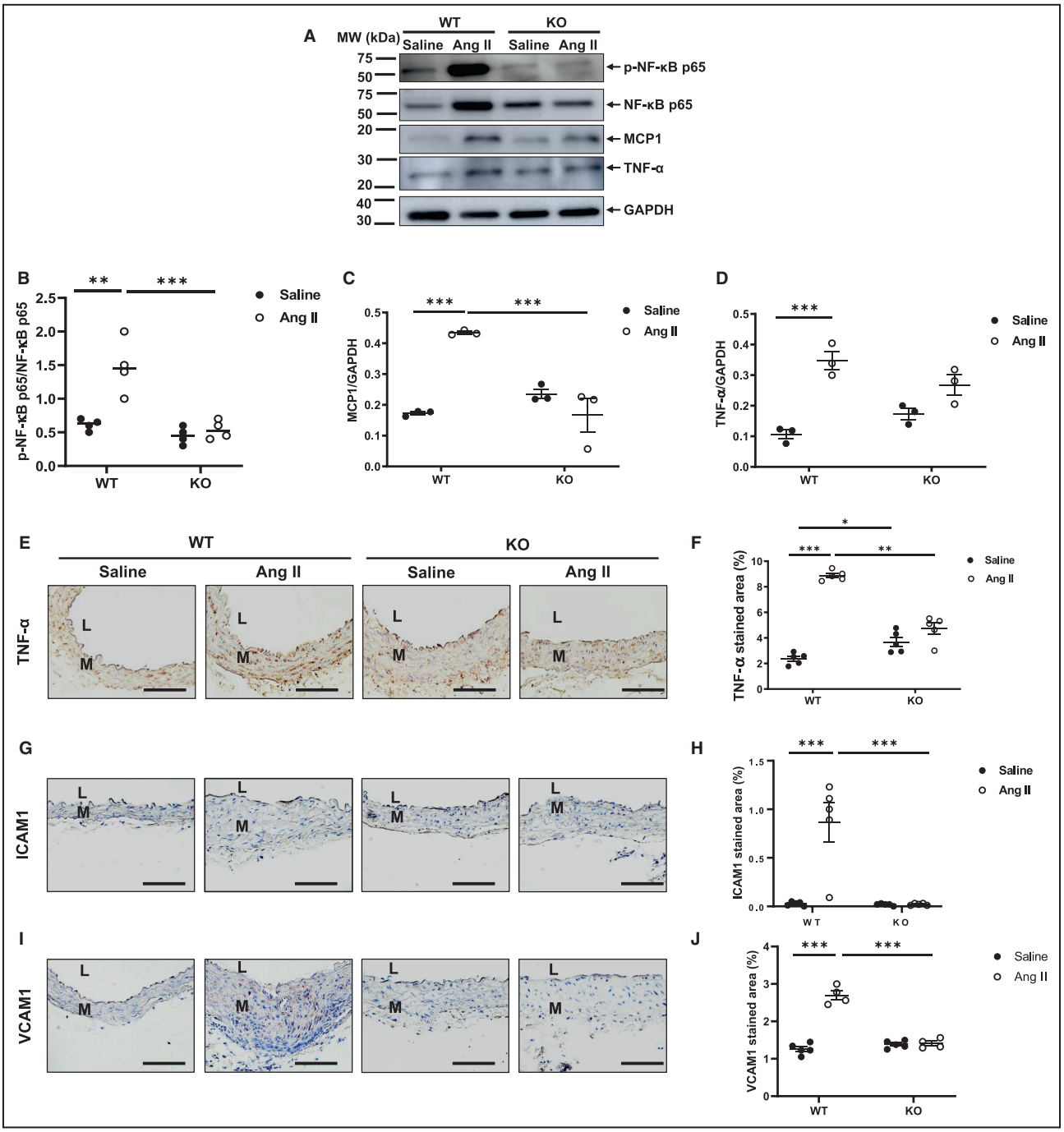

TGF-β1 fibrogenic signaling during adverse arterial remodeling.[22,31]

To determine whether MFG-E8 is *required* for angiotensin II–induced aortic remodeling, we implanted osmotic mini-pumps to infuse either angiotensin II or saline into both MFG-E8 knockout and WT mice at 30 weeks of age. The second major finding of our study was that although circulating levels of angiotensin II increased to even a greater extent in MFG-E8 knockout versus WT mice, aortic IMT in WT mice increased in response to elevations of angiotensin II but did not increase in the MFG-E8 KO. Further, except for a small increase in TGF-β1, there were no significant changes in molecular and cellular mechanisms that underlie adverse age-associated aortic remodeling in response to angiotensin II infusion, including inflammation, MMP2 activation, fibrosis, elastin fragmentation, and VSMCs proliferation[3–6,8,9,13,19,23,32,33] in response to angiotensin II infusion in MFG-E8 knockout mice compared with those in WTmice. Thus, angiotensin II–induced aortic remodeling requires MFG-E8 signaling.

Our results also indicate that increased NF-κB induced inflammation in response to angiotensin II is dependent upon MFG-E8. Angiotensin II treatment markedly

increased p-NF-κB p65, a core element of inflammatory arterial wall remodeling,[34] in MFG-E8 knockout mice but not in WT mice, indicating that MFG-E8 is an essential element in the signaling by which angiotensin II markedly increases NF-κB. Several studies indicate that NF-κB activation facilitates the production of MCP1, TNF-α, ICAM1, and VCAM1 during the processes of arterial inflammation and remodeling[10,25–27,35–39] and that MFG-E8 increases MCP1 activation in VSMCs.[4] In response to angiotensin II infusion, MCP1, TNF-α, ICAM1, and VCAM1 are increased in WT mice but not in MFG-E8–/– KO mice, further indicating that MFG-E8 is a crucial player required for angiotensin II–induced arterial inflammation.

In addition, to the aforementioned proinflammatory factors, the degradation fragment of MFG-E8, medin, per se, induces proinflammatory endothelial activation.[40–42] It is well known that medin is the most common amylogenic protein found in aged arterial walls.[7,13] When angiotensin II induces aortic remodeling, excessive medin fragments may contribute to fibrosis and elastin fragmentation due to a marked increase in MFG-E8.

In summary, our current findings demonstrate that MFG-E8 plays a necessary inflammatory role in age-associated vascular remodeling at the molecular, cellular and tissue levels by promoting increased inflammation, VSMC proliferation, collagen deposition, and elastic fiber fragmentation. Thus, targeting MFG-E8 is a potential molecular approach for the prevention or treatment of adverse arterial remodeling during aging. Supplemental discussion can be found in Data S3.

ARTICLE INFORMATION

Received May 21, 2022; accepted March 24, 2022.

Affiliations

Laboratory of Cardiovascular Science, National Institution on Aging, National Institutes of Health, Biomedical Research Center (BRC), Baltimore, MD (L.N., L.L., W.Z., R.T., J.Z., R.E.M., K.R.M., C.H.M., E.G.L., M.W.); Department of Vascular Surgery, Peking Union Medical College Hospital, Peking Union Medical College & Chinese Academy of Medical Sciences, Beijing, China (L.N., C.L.); Research Center for Molecular Medicine and Chronic Diseases (CIMUS), IDIS, University of Santiago de Compostela, Spain (P.G.-G., J.L.L.-G.); and Networking Research Center on Neurodegenerative Diseases (CIBERNED), Madrid, Spain (P.G.-G., J.L.L.-G.).

Acknowledgments

L.N. and M.W. conceived and designed experiments and wrote the manuscript; L.N., L.L., W.Z., R.T., J.Z., and P.G.G. performed experiments; L.N., L.L., C.H.M., E.G.L., and M.W. analyzed the data; L.N., L.L., C.L., J.L.L, and E.G.L. interpreted results of experiments; L.N. and M.W. wrote the manuscript; R.E.M. and K.R.M. edited the manuscript; and M.W. approved the final version of manuscript.

Sources of Funding

This research was supported by the Intramural Research Program of the National Institute on Aging, National Institutes of Health, the National Natural Science Foundation of China (No. 81470585) and the Fundamental Research Funds for the Central Universities (No. 3332019028).

Disclosures

None.

Supplemental Material

Data S1–S3
Figures S1–S5
References 43–52

REFERENCES

1. Borisenko GG, Iverson SL, Ahlberg S, Kagan VE, Fadeel B. Milk fat globule epidermal growth factor 8 (MFG-e8) binds to oxidized phosphatidylserine: implications for macrophage clearance of apoptotic cells. *Cell Death Differ*. 2004;11:943–945. doi: 10.1038/sj.cdd.4401421
2. Atabai K, Fernandez R, Huang X, Ueki I, Kline A, Li Y, Sadatmansoori S, Smith-Steinhart C, Zhu W, Pytela R, et al. Mfge8 is critical for mammary gland remodeling during involution. *Mol Biol Cell*. 2005;16:5528–5537. doi: 10.1091/mbc.e05-02-0128
3. Wang M, Fu Z, Wu J, Zhang J, Jiang L, Khazan B, Telljohann R, Zhao M, Krug AW, Pikilidou M, et al. MFG-E8 activates proliferation of vascular smooth muscle cells via integrin signaling. *Aging Cell*. 2012;11:500–508. doi: 10.1111/j.1474-9726.2012.00813.x
4. Fu Z, Wang M, Gucek M, Zhang J, Wu J, Jiang L, Monticone RE, Khazan B, Telljohann R, Mattison J, et al. Milk fat globule protein epidermal growth factor-8: a pivotal relay element within the angiotensin ii and monocyte chemoattractant protein-1 signaling cascade mediating vascular smooth muscle cells invasion. *Circ Res*. 2009;104:1337–1346. doi: 10.1161/CIRCRESAHA.108.187088
5. Soubeyrand S, Nikpay M, Turner A, Dang AT, Herfkens M, Lau P, McPherson R. Regulation of MFGE8 by the intergenic coronary artery disease locus on 15q26.1. *Atherosclerosis*. 2019;284:11–17. doi: 10.1016/j.atherosclerosis.2019.02.012
6. Viola JR, Lemnitzer P, Paulin N, Drechsler M, Nazari-Jahantigh M, Maas S, De Jong RJ, Winter J, Schober A, Weber C, et al. Deletion of MFGE8 inhibits neointima formation upon arterial damage. *Thromb Haemost*. 2018;118:1340–1342. doi: 10.1055/s-0038-1649522
7. Wang M, Wang HH, Lakatta EG. Milk fat globule epidermal growth factor VIII signaling in arterial wall remodeling. *Curr Vasc Pharmacol*. 2013;11:768–776.
8. Chiang HY, Chu PH, Lee TH. MFG-E8 mediates arterial aging by promoting the proinflammatory phenotype of vascular smooth muscle cells. *J Biomed Sci*. 2019;26:61. doi: 10.1186/s12929-019-0559-0
9. Ni YQ, Zhan JK, Liu YS. Roles and mechanisms of MFG-E8 in vascular aging-related diseases. *Ageing Res Rev*. 2020;64:101176. doi: 10.1016/j.arr.2020.101176
10. Zhao H, Zhang H, Qin X. Age-related differences in serum MFGE8, TGFBETA1 and correlation to the severity of atherosclerosis determined by ultrasound. *Mol Med Rep*. 2017;16:9741–9748. doi: 10.3892/mmr.2017.7838
11. Degenhardt K, Wagner J, Skodras A, Candlish M, Koppelmann AJ, Wild K, Maxwell R, Rotermund C, von Zweydorf F, Gloeckner CJ, et al. Medin aggregation causes cerebrovascular dysfunction in aging wild-type mice. *Proc Natl Acad Sci USA*. 2020;117:23925–23931. doi: 10.1073/pnas.2011133117
12. Ferrario CM, Strawn WB. Role of the renin-angiotensin-aldosterone system and proinflammatory mediators in cardiovascular disease. *Am J Cardiol*. 2006;98:121–128. doi: 10.1016/j.amjcard.2006.01.059
13. Wang M, Jiang L, Monticone RE, Lakatta EG. Proinflammation: the key to arterial aging. *Trends Endocrinol Metab*. 2014;25:72–79. doi: 10.1016/j.tem.2013.10.002
14. Gromotowicz-Poplawska A, Szoka P, Kolodziejczyk P, Kramkowski K, Wojewodzka-Zelezniakowicz M, Chabielska E. New agents modulating the renin-angiotensin-aldosterone system-will there be a new therapeutic option? *Exp Biol Med (Maywood)*. 2016;241:1888–1899. doi: 10.1177/1535370216660211
15. Wang M, Zhang J, Spinetti G, Jiang LQ, Monticone R, Zhao D, Cheng L, Krawczyk M, Talan M, Pintus G, et al. angiotensiniotensin II activates matrix metalloproteinase type II and mimics age-associated carotid arterial remodeling in young rats. *Am J Pathol*. 2005;167:1429–1442. doi: 10.1016/S0002-9440(10)61229-1
16. Motegi S, Leitner WW, Lu M, Tada Y, Sardy M, Wu C, Chavakis T, Udey MC. Pericyte-derived MFG-E8 regulates pathologic angiogenesis. *Arterioscler Thromb Vasc Biol*. 2011;31:2024–2034. doi: 10.1161/ATVBAHA.111.232587
17. Neutzner M, Lopez T, Feng X, Bergmann-Leitner ES, Leitner WW, Udey MC. MFG-E8/lactadherin promotes tumor growth in an

angiogenesis-dependent transgenic mouse model of multistage carcinogenesis. *Cancer Res*. 2007;67:6777–6785. doi: 10.1158/0008-5472.CAN-07-0165
18. Wang M, Takagi G, Asai K, Resuello RG, Natividad FF, Vatner DE, Vatner SF, Lakatta EG. Aging increases aortic MMP-2 activity and angiotensin II in nonhuman primates. *Hypertension*. 2003;41:1308–1316. doi: 10.1161/01.HYP.0000073843.56046.45
19. Jiang L, Wang M, Zhang J, Monticone RE, Telljohann R, Spinetti G, Pintus G, Lakatta EG. Increased aortic calpain-1 activity mediates age-associated angiotensin II signaling of vascular smooth muscle cells. *PLoS One*. 2008;3:e2231. doi: 10.1371/journal.pone.0002231
20. Verbeke G, Molenberghs G. *A linear mixed models for longitudinal data*. New York: Springer; 2009.
21. Ozasa Y, Akazawa H, Qin Y, Tateno K, Ito K, Kudo-Sakamoto Y, Yano M, Yabumoto C, Naito AT, Oka T, et al. Notch activation mediates angiotensin II-induced vascular remodeling by promoting the proliferation and migration of vascular smooth muscle cells. *Hypertens Res*. 2013;36(10):859–865. doi: 10.1038/hr.2013.52
22. Wang M, Zhao D, Spinetti G, Zhang J, Jiang LQ, Pintus G, Monticone R, Lakatta EG. Matrix metalloproteinase 2 activation of transforming growth factor-beta1 (TGF-beta1) and TGF-beta1-type II receptor signaling within the aged arterial wall. *Arterioscler Thromb Vasc Biol*. 2006;26:1503–1509. doi: 10.1161/01.ATV.0000225777.58488.f2
23. Wang M, Zhang J, Telljohann R, Jiang L, Wu J, Monticone RE, Kapoor K, Talan M, Lakatta EG. Chronic matrix metalloproteinase inhibition retards age-associated arterial proinflammation and increase in blood pressure. *Hypertension*. 2012;60:459–466. doi: 10.1161/HYPERTENSIONAHA.112.191270
24. Wang M, Shah AM. Age-associated pro-inflammatory remodeling and functional phenotype in the heart and large arteries. *J Mol Cell Cardiol*. 2015;83:101–111. doi: 10.1016/j.yjmcc.2015.02.004
25. Wortmann M, Skorubskaya E, Peters AS, Hakimi M, Bockler D, Dihlmann S. Necrotic cell debris induces a NF-kappab-driven inflammasome response in vascular smooth muscle cells derived from abdominal aortic aneurysms (AAA-SMC). *Biochem Biophys Res Commun*. 2019;511:343–349. doi: 10.1016/j.bbrc.2019.02.051
26. Jia Z, Nallasamy P, Liu D, Shah H, Li JZ, Chitrakar R, Si H, McCormick J, Zhu H, Zhen W, et al. Luteolin protects against vascular inflammation in mice and tnf-alpha-induced monocyte adhesion to endothelial cells via suppressing ikappabalpha/nf-kappab signaling pathway. *J Nutr Biochem*. 2015;26:293–302. doi: 10.1016/j.jnutbio.2014.11.008
27. Milstone DS, Ilyama M, Chen M, O'Donnell P, Davis VM, Plutzky J, Brown JD, Haldar SM, Siu A, Lau AC, et al. Differential role of an NF-kappab transcriptional response element in endothelial versus intimal cell VCAM-1 expression. *Circ Res*. 2015;117:166–177. doi: 10.1161/CIRCRESAHA.117.306666
28. Wang M, Fu Z, Lakatta EG, Van Eyk J. Method for the diagnosis of age-associated vascular disorders. European Patent EP2399131. 2012
29. Kim SH, Liu L, Ni L, Zhang L, Zhang J, Wang Y, McGraw KR, Monticone R, Telljohann R, Lakatta EG, et al. MFG-E8 signaling promotes elastolysis and calcification in the aging aortic wall. *bioRxiv*. 2020. doi: 10.1101/2020.10.05.32672
30. Wang M, Kim SH, Monticone RE, Lakatta EG. Matrix metalloproteinases promote arterial remodeling in aging, hypertension, and atherosclerosis. *Hypertension*. 2015;65:698–703. doi: 10.1161/HYPERTENSIONAHA.114.03618
31. Harvey A, Montezano AC, Lopes RA, Rios F, Touyz RM. Vascular fibrosis in aging and hypertension: molecular mechanisms and clinical implications. *Can J Cardiol*. 2016;32:659–668. doi: 10.1016/j.cjca.2016.02.070
32. Spinetti G, Wang M, Monticone R, Zhang J, Zhao D, Lakatta EG. Rat aortic MCP-1 and its receptor CCR2 increase with age and alter vascular smooth muscle cell function. *Arterioscler Thromb Vasc Biol*. 2004;24:1397–1402. doi: 10.1161/01.ATV.0000134529.65173.08
33. Kim SH, Monticone RE, McGraw KR, Wang M. Age-associated proinflammatory elastic fiber remodeling in large arteries. *Mech Ageing Dev*. 2021;196:111490. doi: 10.1016/j.mad.2021.111490
34. Monaco C, Paleolog E. Nuclear factor kappab: a potential therapeutic target in atherosclerosis and thrombosis. *Cardiovasc Res*. 2004;61:671–682. doi: 10.1016/j.cardiores.2003.11.038
35. Ogbozor UD, Opene M, Renteria LS, McBride S, Ibe BO. Mechanism by which nuclear factor-kappa beta (NF-kb) regulates ovine fetal pulmonary vascular smooth muscle cell proliferation. *Mol Genet Metab Rep*. 2015;4:11–18. doi: 10.1016/j.ymgmr.2015.05.003
36. Yu F, Li BY, Li XL, Cai Q, Zhang Z, Cheng M, Yin M, Wang JF, Zhang JH, Lu WD, et al. Proteomic analysis of aorta and protective effects of grape seed procyanidin b2 in db/db mice reveal a critical role of milk fat globule epidermal growth factor-8 in diabetic arterial damage. *PLoS One*. 2012;7:e52541. doi: 10.1371/journal.pone.0052541
37. Cheng M, Li BY, Li XL, Wang Q, Zhang JH, Jing XJ, Gao HQ. Correlation between serum lactadherin and pulse wave velocity and cardiovascular risk factors in elderly patients with type 2 diabetes mellitus. *Diabetes Res Clin Pract*. 2012;95:125–131. doi: 10.1016/j.diabres.2011.09.030
38. Li Y, Ran W, Zhang J, Chen S, Li Y, Luo D, Wang C, Jia W. Circulating milk fat globule-epidermal growth factor 8 levels are increased in pregnancy and gestational diabetes mellitus. *J Diabetes Investig*. 2017;8:571–581. doi: 10.1111/jdi.12616
39. Li Y, Ran W, Zhang J, Chen S, Li Y, Luo D, Wang C, Jia W. Elevated serum milk fat globule-epidermal growth factor 8 levels in type 2 diabetic patients are suppressed by overweight or obese status. *IUBMB Life*. 2017;69:63–71. doi: 10.1002/iub.1592
40. Albus E, Sinningen K, Winzer M, Thiele S, Baschant U, Hannemann A, Fantana J, Tausche AK, Wallaschofski H, Nauck M, et al. Milk fat globule-epidermal growth factor 8 (MFG-E8) is a novel anti-inflammatory factor in rheumatoid arthritis in mice and humans. *J Bone Miner Res*. 2016;31:596–605. doi: 10.1002/jbmr.2721
41. Karamanova N, Truran S, Serrano GE, Beach TG, Madine J, Weissig V, Davies HA, Veldhuizen J, Nikkhah M, Hansen M, et al. Endothelial immune activation by medin: potential role in cerebrovascular disease and reversal by monosialoganglioside-containing nanoliposomes. *J Am Heart Assoc*. 2020;9:e014810. doi: 10.1161/JAHA.119.014810.
42. Migrino RQ, Davies HA, Truran S, Karamanova N, Franco DA, Beach TG, Serrano GE, Truong D, Nikkhah M, Madine J. Amyloidogenic medin induces endothelial dysfunction and vascular inflammation through the receptor for advanced glycation endproducts. *Cardiovasc Res*. 2017;113:1389–1402. doi: 10.1093/cvr/cvx135
43. Garcia-Garrote M, Perez-Villalba A, Garrido-Gil P, Belenguer G, Parga JA, Perez-Sanchez F, Labandeira-Garcia JL, Farinas I, Rodriguez-Pallares J. Interaction between angiotensin type 1, type 2, and mas receptors to regulate adult neurogenesis in the brain ventricular-subventricular zone. *Cells*. 2019;8:1551. doi: 10.3390/cells8121551
44. Ito M, Oliverio MI, Mannon PJ, Best CF, Maeda N, Smithies O, Coffman TM. Regulation of blood pressure by the type 1a angiotensin II receptor gene. *Proc Natl Acad Sci USA*. 1995;92:3521–3525. doi: 10.1073/pnas.92.8.3521
45. Ichiki T, Labosky PA, Shiota C, Okuyama S, Imagawa Y, Fogo A, Niimura F, Ichikawa I, Hogan BL, Inagami T. Effects on blood pressure and exploratory behaviour of mice lacking angiotensin II type-2 receptor. *Nature*. 1995;377:748–750. doi: 10.1038/377748a0
46. Lin YP, Hsu ME, Chiou YY, Hsu HY, Tsai HC, Peng YJ, Lu CY, Pan CY, Yu WC, Chen CH, et al. Comparative proteomic analysis of rat aorta in a subtotal nephrectomy model. *Proteomics*. 2010;10:2429–2443. doi: 10.1002/pmic.200800658
47. Lau SY, Barrett CJ, Guild SJ, Chamley LW. Necrotic trophoblast debris increases blood pressure during pregnancy. *J Reprod Immunol*. 2013;97:175–182. doi: 10.1016/j.jri.2012.12.005
48. Deng KQ, Li J, She ZG, Gong J, Cheng WL, Gong FH, Zhu XY, Zhang Y, Wang Z, Li H. Restoration of circulating MFGE8 (milk fat globule-EGF factor 8) attenuates cardiac hypertrophy through inhibition of akt pathway. *Hypertension*. 2017;70:770–779. doi: 10.1161/HYPERTENSIONAHA.117.09465
49. Ge Z, Chen Y, Wang B, Zhang X, Yan Y, Zhou L, Zhang Y, Xie Y. MFGE8 attenuates angiotensin-II-induced atrial fibrosis and vulnerability to atrial fibrillation through inhibition of TGF-Beta1/Smad2/3 pathway. *J Mol Cell Cardiol*. 2020;139:164–175. doi: 10.1016/j.yjmcc.2020.01.001
50. Wang B, Ge Z, Wu Y, Zha Y, Zhang X, Yan Y, Xie Y. MFGE8 is down-regulated in cardiac fibrosis and attenuates endothelial-mesenchymal transition through Smad2/3-Snail signalling pathway. *J Cell Mol Med*. 2020;24:12799–12812. doi: 10.1111/jcmm.15871
51. Deroide N, Li X, Lerouet D, Van Vre E, Baker L, Harrison J, Poittevin M, Masters L, Nih L, Margaill I, et al. MFGE8 inhibits inflammasome-induced il-1beta production and limits postischemic cerebral injury. *J Clin Invest*. 2013;123:1176–1181. doi: 10.1172/JCI65167
52. Khalifeh-Soltani A, McKleroy W, Sakuma S, Cheung YY, Tharp K, Qiu Y, Turner SM, Chawla A, Stahl A, Atabai K. MFGE8 promotes obesity by mediating the uptake of dietary fats and serum fatty acids. *Nat Med*. 2014;20:175–183. doi: 10.1038/nm.3450

SUPPLEMENTAL MATERIAL

Data S1. Supplemental Materials and Methods

Experimental Animals

30-week-old male MFG-E8 KO mice and age-matched WT mice were used in this Ang II infusion study. In addition, 4-, 8-, 20, 50-, and 96-week-old male WT and age-matched KO paraffin archival aortic sections or frozen tissue (in graphs, individual data represents the number of the aortic samples) were employed for the study of age-related arterial remodeling. 10-week-old WT and age-matched KO were utilized for measuring circulating triglyceride, cholesterol, and glucose.

10-week-old male WT, AT1, and AT2 receptor knock out mice (WT, AT1 and AT2 KO, respectively) were provided by Professor Jose Luis Labandeira-Garcia. [43] Mice carrying genetic deletions of the Agtr1 (AT1 KO) gene were obtained from The Jackson Laboratory (Bar Harbor, ME, USA) and Agt2 mice (AT2-KO were generously donated by Dr. Daniel Henrion (University of Angers, Angers, France). [44, 45]

Blood Pressure Measurement

SBP was measured using the pneumatic tail-cuff method (MRBP System, Life Science, Woodland Hills, California). Briefly, animals were placed in a plastic chamber maintained at 34°C and a cuff with a pneumatic pulse sensor was attached to the tail for SBP measurements. Mice were trained for one week to become accustomed to the new handling and environment. Once SBP values were consistent, eight consecutive measurements were performed for each mouse and all the values collected were averaged. Blood pressure was monitored 1 week prior to mini-pump implantation (baseline), and once per week from day 7 to 28 after minipump implantation.

Analysis of Circulating Total Cholesterol, Triglycerides, and Glucose in Untreated WT and KO Mice

Six male 10-weeks-old MFG-E8 KO (KO) and 6 age-matched WT mice were fasted for 16 hours before sacrifice. The mice were anaesthetized via intraperitoneal injection with ketamine (100 mg/kg of body weight) and xylazine (5 mg/kg per body weight). The thoracic cavity was accessed by cutting the sternum to expose the heart, after a 22 G needle attached to a 3 mL syringe was used to puncture the apex of the heart and 800-1,000 µL of blood was collected, representing most of the animal's total blood volume, and was expected to be arterial blood. Blood was collected in heparin tubes (BD, Franklin Lakes NJ, Item# 36664) and placed on ice for 15 minutes. Samples were then spun down at 10,000 rpm for 10 minutes and plasma was harvested and stored at −80°C until use. Total cholesterol, triglycerides and glucose levels were measured from plasma samples according to manufacturer instructions. Assay kits for cholesterol (item# 234-60, lot# 54416), triglycerides (item# 236-660, Lot# 54604) and glucose (item# 235-60, lot# 53909) were obtained from Sekure diagnostics (One Wall Street Burlington, MA 01803 USA), and measured using the Cobas Fara II (Roche Diagnostics Roche Diagnostics Corporation 9115 Hague Rd Indianapolis, IN 46256 USA) chemical analyzer.

Morphometric Analysis of Aortic Walls in Untreated Aging WT and KO Mice

We measured intimal medial thickening (IMT) with aging, by staining archival aortic paraffin sections with hematoxylin and eosin (H&E) from untreated 20-week-old young (WT: n=44; KO: n=40) and 96-week-old aged mice (WT: n=39; KO: n=40). The local renin angiotensin system, including Ang II, AT1 and AT2 receptors, and NF-κB activation, were measured in 8-week-old young (WT: n=4; KO: n=5) and 50-week-old aged mice (WT: n=4; MFG-E8 KO: n=4) using immunohistostaining and Western blotting analyses.

Data S2. Supplemental Results

Ang II, AT1, AT2, and NF-κB Expression in the Arterial wall in Aging Mice

Aortic Ang II protein was significantly increased in untreated aging WT mice, but in the MFG-E8 KO this effect was significantly reduced (**Figure S1A**).

In addition, immunostaining demonstrated that the Ang II receptor AT1 was markedly increased in the aortic walls of untreated WT 96- versus 4-week-old, but the absence of MFG-E8 significantly reduced this age effect; and the Ang II receptor AT2 was markedly decreased in aging WT aortic walls, but the absence of MFG-E8 diminished these effects (**Figure S1B & 1C**). Western blot analysis further confirmed the aging effect on AT1 and AT2 expression (50- versus 8-week-old) (**Figure 1D**).

In addition, Western blotting analysis of aortic protein from 10-week-old male AT1 and AT2 receptor knock out mice indicated that aortic MFG-E8 protein levels were significantly decreased in AT1 KO, but these levels were not altered in AT2 KO mice (**Figure S2**).

NF-κB p65 Expression with Age is Dependent on MFG-E8

Interestingly, immunostaining and Western blotting analysis demonstrated that aging markedly increased the master inflammatory transcription factor p-NF-κB p65 in WT, but MFG-E8 deficiency significantly alleviated this age effect (**Figure S3**).

Ang II Infusion Increases SBP in mice

Increased SBP induced by Ang II infusion was observed in all mice. The repeated, two-way ANOVA analysis showed that SBP had a statistically significant of treatment x genotype interaction ($p<0.0001$) (**Figure S4A).** At baseline (time=day 0) there was no significant difference

in SBP among any of the groups. However, after Ang II infusion, both WT and KO, showed significantly increased SBP levels compared to saline infused mice. Unexpectedly, in KO, the SBP of Ang II infused mice was significantly elevated compared to WT after the infusion ($p<0.01$); and similarly, in KO, the SBP of saline infused was also significantly elevated compared to WT after the infusion ($p<0.01$) **(Figure S4A)**. However, the percentage change of the SBP after Ang II infusion was not significantly altered in KO vs WT (**Figure S4B**), suggesting that Ang II infusion produced a similar hypertensive effect.

Circulating Cholesterol, Triglyceride, and Glucose Profile in Mice

In addition, the baseline blood test results from 10-week-old male WT and KO mice showed that the absence of MFG-E8 significantly decreased plasma cholesterol and triglyceride levels but did not alter plasma glucose levels (**Figure S5**), suggesting that MFG-E8 is involved in lipid metabolism.

Data S3. Supplemental Discussion

Ang II signaling effects on the expression of MFG-E8 during age-associated inflammatory remodeling in mice. The AT1 receptor promotes Ang II inflammatory events while the AT2 receptor blocks Ang II induced inflammation. [43-45] Ang II and AT1 were increased while AT2 was decreased during adverse arterial remodeling in aging mice and was dependent on MFG-E8 (**Figure S1**). Ang II infusion increased the AT1 receptor abundance while it decreased AT2 expression in the arterial wall in mice, which was alleviated by the absence of MFG-E8. In addition, MFG-E8 protein levels were markedly decreased in the AT1 KO mice but are not in the AT2 KO when compared to WT (**Figure S2**). Notably, aging markedly increased the master inflammatory transcription factor p-NF-κB p65 in WT, but MFG-E8 deficiency significantly

alleviated this age effect (**Figure S3**). These findings suggest that the Ang II signaling cascade impacts MFG-E8 expression mainly through the AT1 receptor during age-associated inflammatory remodeling in mice.

Ang II signaling is a key molecular event of age-associated arterial intimal medial thickening. [4, 15,18,19] In the current study, Ang II infusion markedly increased IMT in young WT but not in young KO mice compared to saline infused animals; aging increased IMT in the WT but not in the KO mice; and aging also increased Ang II/AT1 receptor protein expression in the WT but no in the KO animals. These findings indicate that MFG-E8 is required for Ang II-associated vascular intimal medial thickening with aging. Unexpectedly, the KO mice infused with saline had higher levels of IMT than the WT saline control (**Figure 3A**). Notably, at the start of saline infusion, no difference in SBP was observed between the 30-week-old KO and WT animals; however, during the last two weeks of the experiment, SBP levels of the KO animals became elevated when compared to the WT saline (**Figure S4A**). The increased SBP levels during saline infusion could help explain the elevated levels of IMT in the saline infused KO versus WT mice.

MFG-E8 impacts blood pressure in mice. Aortic MFG-E8 is increased in renal hypertensive rats. [46] Increased MFG-E8 is colocalized with increased Ang II protein within old human aortic walls. [4] Ang II infusion increased MFG-E8 in the aortae of mice. These findings suggest that MFG-E8 may influence Ang II associated blood pressure increases. The current study indicated that SBP was increased over a 28-day time course in 30-week-old KO versus WT mice after saline infusion; similarly, SBP was also increased over a 28-day time course in 30-week-old KO versus WT animals after Ang II infusion (**Figure S4A**). However, the percentage change of SBP was not altered in KO versus WT after Ang II infusion (**Figure S4B).** It is well-known that MFG-E8 is a bridging molecule for the clearance of cellular debris by macrophages, and the

absence of MFG-E8 impairs the cleanup of cellular debris, which accumulate and may potentially increase blood pressure in mice. [47] In addition, aging increases MFG-E8 and increases its small, cleaved fragment medin, [7,13,41,42] which is the most common amylogenic protein in aged arterial walls and may potentially induce inflammation and blood pressure increases in old mice.

The inflammatory role of MFG-E8 in the cardiovascular system. There is an apparent contradiction of our current findings which show MFG-E8 promotes an inflammatory role in the arterial wall compared to previous findings which suggests that MFG-E8 exerts an anti-inflammatory role in the heart. [48-50] For example, MFG-E8 attenuates Ang-II induced atrial fibrosis and atrial fibrillation through the inhibition of the TGF-β1/Smad2/3 pathway. [49] MFG-E8 allevaites ventricle fibrosis via the attenuation of endothelial-mesenchymal transition through the Smad2/3/snail signalling pathway. [50] Importantly, restoring circulating MFG-E8 levels retards cardiac hypertrophy through the inhibition of the Akt (protein kinase B, PKB) pathway. [48] In addition, MFG-E8 signaling impacts on adaptive immunity, including the role of anti-inflammation in postischemic cerebral injury. [51] The underlying mechanisms of the inflammatory discrepancies between the heart and arteries is unknown, which need to be further studied.

MFG-E8 is involved in metabolism. MFG-E8 deficiency significantly decreased cholesterol and triglyceride levels (**Figure S5**). The absence of MFG-E8 has been shown to impede the development of obesity by inhibiting the uptake of dietary fat and serum fatty acids in mice. [52] Notably, circulating levels of Ang II post-infusion are significantly higher in KO than WT animals, suggesting that MFG-E8 may be involved in the metabolism of Ang II. The underlying mechanism of MFG-E8-associated metabolism needs to be further investigated.

Supplemental Figures

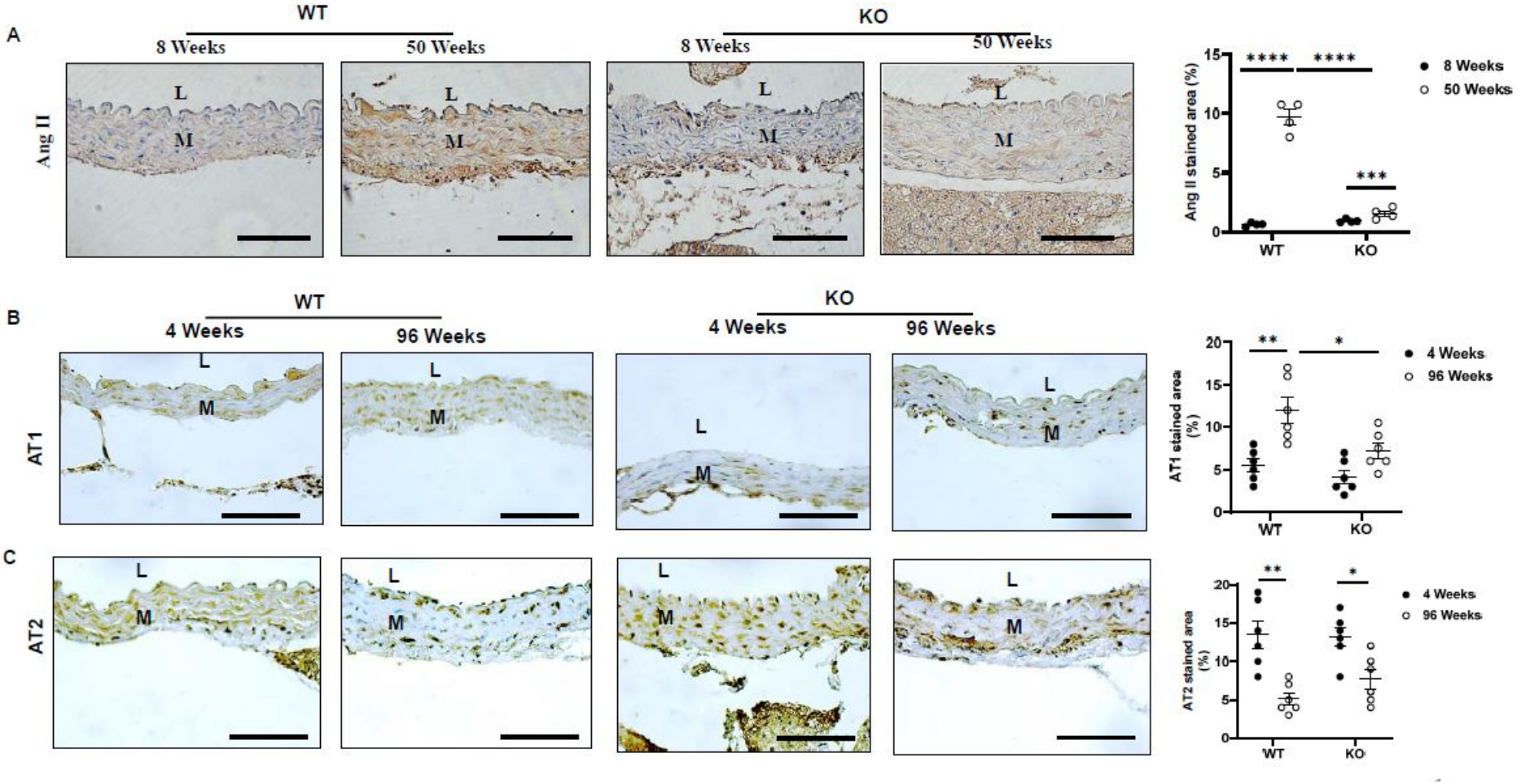

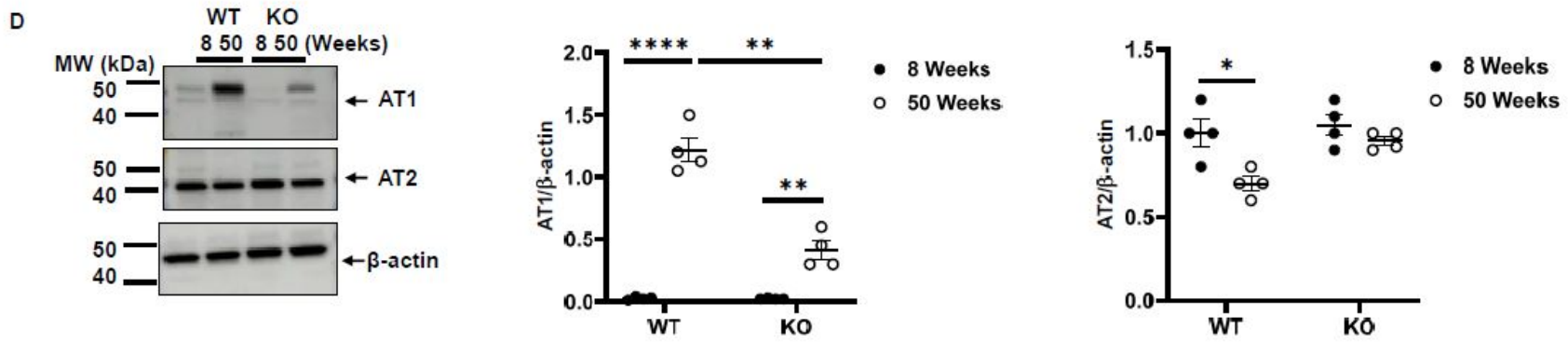

Figure S1. Ang II and AT1/AT2 Expression During Age-Associated Inflammatory Remodeling in Mice. A. Representative photomicrographs of immunostaining of aortic Ang II. Morphometric analysis of Ang II immunostaining in the aortic wall shows Ang II abundance ($p<0.0001$ for main age effect, $p<0.0001$ for main genotype effect, $p<0.0001$ for age x genotype, by two-way ANOVA). Graph showing mean ± SEM combined with individual data points for KO and WT mice. ***=$p<0.001$; and ****=$p<0.0001$ by Bonferroni post-hoc tests following two-way ANOVA. L=lumen; M=media. Scale bar = 100μm. **B.** Representative photomicrographs of immunostaining of the Ang II AT1 receptor. Morphometric analysis of the AT1 immunostaining in the aortic wall ($p<0.01$ for main age effect, $p<0.001$ for main genotype effect, by two-way ANOVA). Graph showing mean ± SEM combined with individual data points for KO and WT mice. *=$p<0.05$ and **=$p<0.01$ by Bonferroni post-hoc tests following two-way ANOVA. **C.** Representative photomicrographs of immunostaining of the aortic Ang II AT2 receptor. Morphometric analysis of AT2 abundance ($p<0.0001$ for main age effect, by two-way ANOVA). Graph showing mean ± SEM combined with individual data points for KO and WT mice. *=$p<0.05$ and **=$p<0.01$ by Bonferroni post-hoc tests following two-way ANOVA. **D.** Representative Western blots of the AT1 and AT2

receptors (left panels). Western blotting analysis of the AT1 abundance ($p<0.0001$ for main age effect, $p<0.0001$ for main genotype effect, $p<0.0001$ for age x genotype, by two-way ANOVA). Graph (middle panel) showing mean ± SEM combined with individual data points for KO and WT mice. **=$p<0.01$and ****=$p<0.0001$ by Bonferroni post-hoc tests two-way ANOVA. Western blotting analysis of the AT2 abundance (right panel) ($p<0.05$ for main age effect, $p<0.01$ for main genotype effect, by two-way ANOVA). Graph showing mean ± SEM combined with individual data points for KO and WT mice. *=$p<0.05$ by Bonferroni post-hoc tests following two-way ANOVA. L=lumen; M=media. Scale bar = 100 μm.

Figure S2. Effects of Ang II receptors on MFG-E8 expression in the aortic wall of mice. Representative Western blots (left panel) of aortic MFG-E8 from 10-week-old AT1 and AT2 KO mice. Western blotting analysis of MFG-E8 abundance ($p<0.001$ for the genotype effect, by one-way ANOVA). Graph (right panel) showing mean ± SEM combined with individual data points for KO and WT mice. ****=$p<0.0001$ by Bonferroni post-hoc tests following one-way ANOVA.

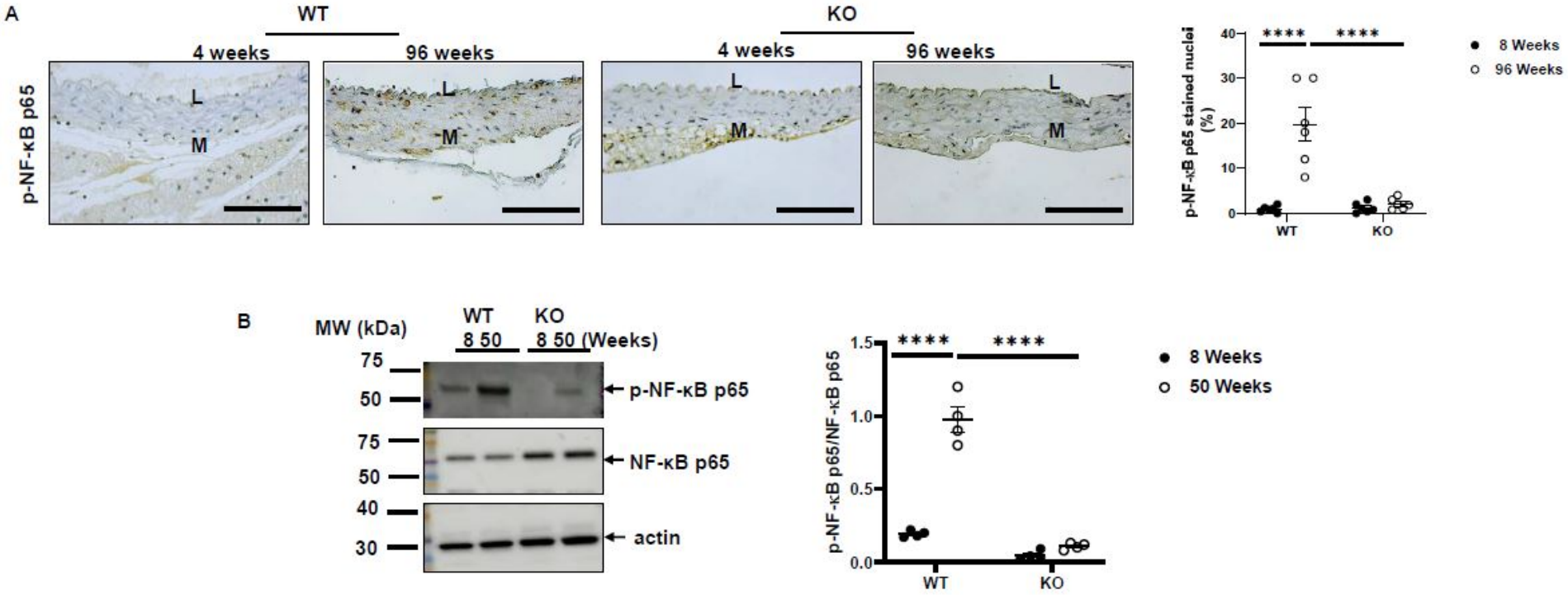

Figure S3. The age-associated activation of NF-κB in the aortic wall of mice. A. Representative photomicrographs of immunostaining of aortic p-NF-κB p65. Morphometric analysis of the percentage of p-NF-κB p65 stained nuclei in the aortic wall ($p<0.001$ for main age effect, $p<0.0001$ for main genotype effect, $p<0.001$ for age x genotype, by two-way ANOVA). Graph showing mean ± SEM combined with individual data points for KO and WT mice. ****=$p<0.0001$ by Bonferroni post-hoc tests following two-way ANOVA. **B.** Representative Western blots of NF-κB p65 (left panel). Western blotting analysis of the p-NF-κB p65 abundance

($p<0.0001$ for main age effect, $p<0.0001$ for main genotype effect, $p<0.0001$ for age x genotype, by two-way ANOVA). Graph (right panel) showing mean ± SEM combined with individual data points for KO and WT mice. *=$p<0.05$ and ****=$p<0.0001$ by Bonferroni post-hoc tests following two-way ANOVA. L=lumen; M=media. Scale bar = 100 μm.

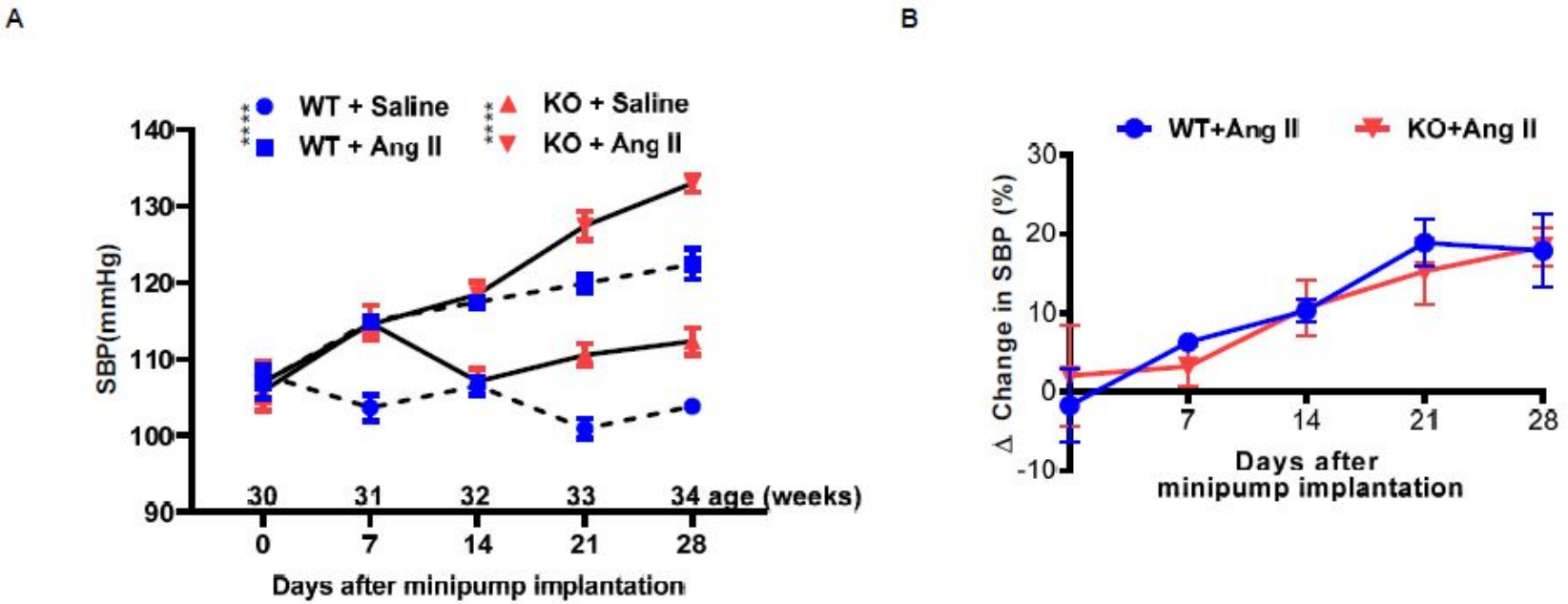

Figure S4. Dynamic changes in systolic blood pressure in mice. A. Dynamic changes in mouse SBP measured by tail-cuff method; plot shows mean ± SEM for KO and WT mice (n=5/group) with Ang II or saline infusion over time ($p<0.001$ for main treatment effect, $p<0.001$ for main genotype effect, $p<0.001$ for Ang II infusion x genotype, by repeated two-way ANOVA and a linear mixed-effects model). ****=$p<0.0001$ SBP in KO + Ang II vs KO + saline and WT + Ang II vs WT + saline group. **B**. Dynamic percentage changes in mouse SBP as measured by tail-cuff method; graph showing mean ± SEM for KO and WT mice (n=5/group) with Ang II or saline infusion over time, $p>0.05$, analyzed by repeated two-way ANOVA.

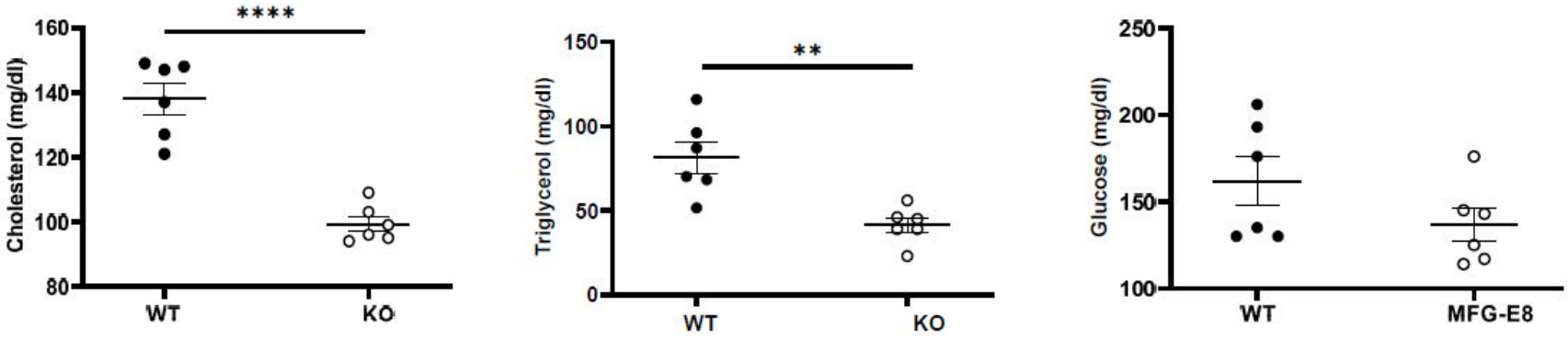

Figure S5. Circulating cholesterol, triglyceride, and glucose in mice. Plasma cholesterol (left panel), triglyceride (middle panel), and glucose (right panel). Graph showing mean ± SEM combined with individual data points for KO and WT mice. ** =$p<0.01$ and ****=$p<0.0001$ by unpaired t-test.